Non-Data-Aided Carrier Offset Estimators for OFDM With Null Subcarriers: Identifiability, Algorithms, and Performance

Xiaoli Ma, Cihan Tepedelenlioğlu, *Member, IEEE*, Georgios B. Giannakis, *Fellow, IEEE*, and Sergio Barbarossa, *Member, IEEE*

***Abstract*—The ability of orthogonal frequency-division multiplexing systems to mitigate frequency-selective channels is impaired by the presence of carrier frequency offsets (CFOs). In this paper, we investigate identifiability issues involving high-resolution techniques that have been proposed for blind CFO estimation based on null subcarriers. We propose new approaches that do not suffer from the lack of identifiability and adopt adaptive algorithms that are computationally feasible. The performance of these techniques in relation to the location of the null subcarriers is also investigated via computer simulations and compared with the modified Cramér–Rao bound.**

***Index Terms*—Estimation, modified Cramér–Rao bound, multicarrier transmission, orthogonal frequency-division multiplexing (OFDM), synchronization.**

I. Introduction

ORTHOGONAL frequency division multiplexing (OFDM) enables high data-rate transmissions over frequency-selective channels at low complexity. It has been chosen for the European digital audio and video broadcasting standards, as well as for the wireless local-area networking standards IEEE802.11a and HIPERLAN/2. Relying on multiple orthogonal subcarriers, OFDM systems turn the frequency-selective fading channel into a set of parallel flat-fading subchannels, which makes them well suited for high-speed transmissions over channels with long delay spreads. However, the presence of a carrier frequency offset (CFO) destroys the orthogonality among subcarriers, and the resulting intercarrier interference degrades the bit error rate (BER) performance severely [17]. Thus, estimation and removal of the CFO from the received data is most critical in OFDM systems and has received considerable attention in recent years.

The extensive literature on CFO estimation for OFDM can be categorized as data-aided schemes (e.g., [14] and [18]) and non-data-aided (blind) schemes that only rely on the received OFDM symbols (see, e.g., [1]–[3], [10]–[12], [15], and [20]. A training method based on the transmission of an OFDM symbol with identical halves is proposed in [18]. The CFO acquisition range of [18] is extended in [14] by using one training symbol with more than two identical parts. A blind method is developed in [15] along with a maximum likelihood CFO estimator based on two consecutive and identical received blocks, where the estimable CFO is restricted to less than half of the subcarrier spacing. CFO estimators that exploit the cyclic prefix are summarized in [9], which also presents a minimum variance unbiased CFO estimator.

Although the ease in handling *frequency-selective* channels constitutes OFDM's primary success factor, most blind CFO estimators deal with *frequency-nonselective* (pure delay) channels [2], [3], [9]. The generalization of cyclic CFO estimators to frequency-selective channels is given in [12]. Subspace-based approaches that rely on the insertion of null (or virtual) subcarriers at the transmitter are derived in [3], [10], and [20], but the effect of frequency selectivity on the identifiability and performance is not addressed. These methods, as well as those in [4] and [8], do not assure identifiability (and thus consistency) of the resulting CFO estimators regardless of the underlying channel nulls. Null subcarriers are also exploited in [1] for synchronization of single- and multiuser multicarrier systems. Hopping the null subcarrier locations from block to block renders the performance independent of the channel zero locations [1].

In this paper, we thoroughly study the effects of the frequency-selective channel on the identifiability and performance of non-data-aided schemes for single-user OFDM with null subcarriers. In Section II, we develop a matrix-vector model for the OFDM system in baseband with null subcarriers and a possible frequency offset. Section III shows that placing null subcarriers consecutively results in a covariance matrix of the received data that might not uniquely determine the CFO in the presence of channel nulls. The same section also discusses the implications of nonuniqueness to MUSIC-based [10] and ESPRIT-based [20] schemes. Section IV solves this identifiability problem by proposing the following alternatives: 1) spacing the null subcarriers in a judicious nonconsecutive way, 2) making the location of the null subcarriers dependent on the OFDM block index (which is referred to as "subcarrier hopping"), or 3) combining subcarrier hopping with consecutively placed null subcarriers. Section IV also proves that 1)–3) guarantee identifiability. In Section V, we adopt the adaptive algorithms of [1] to offer online CFO estimators based on 1)–3). Section VI

Manuscript received February 1, 2001; revised July 30, 2001. This work was supported by the NSF Wireless Initiative under Grant 9979443. Part of this work was presented at the Third IEEE Workshop on Signal Processing Advances in Wireless Communications, Taiwan, R.O.C., March 20–23, 2001.

X. Ma and G. B. Giannakis are with the Department of Electrical and Computer Engineering, University of Minnesota, Minneapolis, MN 55455 USA (e-mail: xiaoli@ece.umn.edu; georgios@ece.umn.edu).

C. Tepedelenlioğlu is with the Department of Electrical Engineering, Arizona State University, Tempe, AZ 85287 USA (e-mail: cihan@asu.edu).

S. Barbarossa is with the INFOCOM Department, University of Rome "La Sapienza," 00184 Rome, Italy (e-mail: sergio@infocom.uniroma1.it).

Publisher Item Identifier S 0733-8716(01)10298-2.

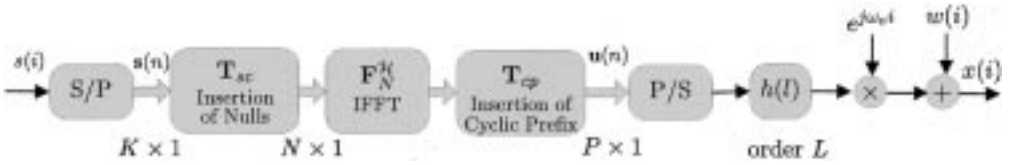

Fig. 1. Discrete-time equivalent baseband model.

provides analytical and simulated performance comparisons, and Section VII concludes this paper.

Upper (lower) boldface letters will be used for matrices (column vectors). Superscript $\mathcal{H}$ will denote Hermitian, $*$ conjugate, $\Re(\cdot)$ real part, $\Im(\cdot)$ imaginary part, T transpose, $\dagger$ pseudoinverse, and $\star$ convolution. We will reserve $E[\cdot]$ for expectation with respect to all the random variables within the brackets, and $\mathcal{R}(\cdot)$ and $\mathcal{N}(\cdot)$ for the range space and null space of a matrix, respectively. The expression $z = y \bmod x$ yields the smallest $z \geq 0$ such that $y = nx + z$ for some nonnegative integer n. We will use $[\mathbf{A}]_{k,m}$ to denote the (k, m)th entry of a matrix $\mathbf{A}$ and $[\mathbf{x}]_m$ to denote the mth entry of vector $\mathbf{x}$; $\mathbf{I}_N$ will denote the $N \times N$ identity matrix; $\mathbf{e}_i$ the $(i+1)$st column of $\mathbf{I}_N$; $[\mathbf{F}_N]_{m,n} := N^{-(1/2)} \exp(-j2\pi mn/N)$ the $N \times N$ fast Fourier transform (FFT) matrix; and $\mathbf{0}_{N\times M}$ the all-zero matrix of dimensions $N \times M$. We define $\mathbf{f}_N(\omega) := [1, \exp(j\omega), \ldots, \exp(j(N-1)\omega)]^T$. $\mathbf{D}_N(\mathbf{h})$ with a vector argument will denote an $N \times N$ diagonal matrix with $[\mathbf{D}_N(\mathbf{h})]_{n,n} = [\mathbf{h}]_n$. For a diagonal matrix with a Vandermonde vector on its diagonal, we will just use a scalar argument: $\mathbf{D}_N(\omega) := \mathbf{D}_N(\mathbf{f}_N(\omega))$.

II. Block System Model

In this section, we will develop a matrix-vector model for a discrete-time-equivalent OFDM system in baseband with null subcarriers, taking the possible presence of the CFO into account. The resulting block model will prove useful for the purposes of studying the identifiability and performance of CFO estimators in the presence of nonideal frequency-selective channel effects. Hence, in what follows, we will extend the matrix-vector OFDM model in [22] to the case where a CFO is present.

Consider the discrete-time equivalent baseband model of the block transmission system depicted in Fig. 1, where the information stream $s(n)$ is drawn from a finite alphabet and parsed into blocks of length K. The nth block is denoted as $\mathbf{s}(n) := [s(nK), s(nK+1), \ldots, s(nK+K-1)]^T$. After the serial-to-parallel (S/P) conversion, zeros are inserted into $\mathbf{s}(n)$ to obtain a longer $N\times 1$ vector with $N > K$. We will denote the indexes of the inserted zeros as $i_1 < \cdots < i_{N-K}$ and the remaining K indexes as $\bar{i}_1 < \cdots < \bar{i}_K$, so that $\{i_k\}_{k=1}^{N-K} \cup \{\bar{i}_k\}_{k=1}^{K} = \{0, \ldots, N-1\}$. The insertion of zeros can be represented analytically by a null subcarrier insertion matrix $\mathbf{T}_{\rm sc} := [\mathbf{e}_{\bar{i}_1} \cdots \mathbf{e}_{\bar{i}_K}]$. When $\mathbf{T}_{\rm sc}$ premultiplies the $\mathbf{s}(n)$ block, it yields an $N\times 1$ vector with zeros in the entries given by $\{i_k\}_{k=1}^{N-K}$. For OFDM transmission, the $N\times 1$ vector $\mathbf{T}_{\rm sc}\mathbf{s}(n)$ is left multiplied by the $N\times N$ inverse FFT (IFFT) matrix $\mathbf{F}_N^{\mathcal{H}}$, which implements the N-point IFFT of $\mathbf{T}_{\rm sc}\mathbf{s}(n)$.

To compensate for the channel's time-dispersive effects, a cyclic prefix (CP) is inserted subsequently. Mathematically, the CP operation is represented by the matrix $\mathbf{T}_{\rm cp} := [(\mathbf{I}_{\overline{L}\times N})^T\, \mathbf{I}_N^T]^T$, where $\overline{L}$ is the length of the CP, which is an upper bound to the channel order $L \leq \overline{L}$; and $\mathbf{I}_{\overline{L}\times N}$ consists of the last $\overline{L}$ rows of $\mathbf{I}_N$. The resulting transmitted block has length $P = N + \overline{L}$ and is given by

$$\mathbf{u}(n) = \mathbf{T}_{\rm cp}\mathbf{F}_N^{\mathcal{H}}\mathbf{T}_{\rm sc}\mathbf{s}(n). \tag{1}$$

Each block $\mathbf{u}(n)$ is serialized for transmission through the possibly unknown time-invariant frequency-selective channel, which in discrete-time equivalent form has finite impulse response $h(l)$ of order L. This is given by $h(l) = g^{(\rm tr)}(t) \star h^{(\rm pr)}(t) \star g^{(\rm rec)}(t)|_{t=lT-\tau_0}$, where $\star$ denotes convolution; $g^{(\rm tr)}(t)$ is the transmitter pulse shape; $h^{(\rm pr)}(t)$ is the impulse response of the propagation medium in continuous time; $g^{(\rm rec)}(t)$ is the receive filter; T is the sampling period; and τ_0 is the combined timing offset/propagation delay. The receiver filter $g^{(\rm rec)}(t)$ is selected to have square-root Nyquist characteristics so that white noise at its input remains white at its output. In the presence of a frequency offset $\overline{\omega}_o$, the samples at the receive filter output are (see also Fig. 1)

$$x(i) = e^{j\omega_o i} \sum_{l=0}^{L} h(l)u(i-l) + w(i) \tag{2}$$

where $\omega_o := \overline{\omega}_o T$ is the normalized CFO, which could be due to Doppler effects or mismatch between the transmitter and receiver oscillators; $u(nP+p)$ is the serialized version of the nth block $\mathbf{u}(n)$ with pth entry $[\mathbf{u}(n)]_p = u(nP+p)$; and $w(i)$ denotes zero-mean additive white Gaussian noise (AWGN) that is assumed to be independent of $\mathbf{s}(n)$.

Selecting our OFDM block size greater than the channel order ($P > L$) implies that each received block $\mathbf{x}(n)$ depends only on two consecutive transmitted blocks $\mathbf{u}(n)$ and $\mathbf{u}(n-1)$, which is referred to as interblock interference (IBI) or as inter-OFDM-symbol interference. At the receiver, we form $P\times 1$ blocks $\mathbf{x}(n)$, which after using (2) can be expressed as (see also [12] and [22])

$$\mathbf{x}(n) = e^{j\omega_o nP}\mathbf{D}_P(\omega_o)[\mathbf{H}_0\mathbf{u}(n) + \mathbf{H}_1\mathbf{u}(n-1)] + \mathbf{w}(n) \tag{3}$$

where $[\mathbf{x}(n)]_p := x(nP+p)$, and likewise for $\mathbf{w}(n)$. Channel matrices $\mathbf{H}_0$ and $\mathbf{H}_1$ are $P \times P$ lower and upper triangular Toeplitz, respectively. $\mathbf{H}_0$'s first column is $[h(0), \ldots, h(L), 0, \ldots, 0]^T$ and $\mathbf{H}_1$'s first row is $[0, \ldots, 0, h(L), \ldots, h(1)]$.

Discarding the CP at the receiver amounts to removing the first $\overline{L}$ elements of $\mathbf{x}(n)$ in (3). This is accomplished through the CP removing matrix $\mathbf{R}_{\rm cp} := [\mathbf{0}_{N\times\overline{L}}\mathbf{I}_N]$ that yields $\mathbf{y}(n) := \mathbf{R}_{\rm cp}\mathbf{x}(n)$. Substituting directly from the definitions of $\mathbf{R}_{\rm cp}$ and $\mathbf{H}_1$, it follows readily that $\mathbf{R}_{\rm cp}\mathbf{H}_1 = \mathbf{0}_{N\times P}$. Furthermore, one can confirm that $\mathbf{R}_{\rm cp}\mathbf{D}_P(\omega_o) = e^{j\omega_o\overline{L}}\mathbf{D}_N(\omega_o)\mathbf{R}_{\rm cp}$. Using (3) and the expression for $\mathbf{u}(n)$ from (1),

defining $\mathbf{H} := \mathbf{R}_{\rm cp}\mathbf{H}_0\mathbf{T}_{\rm cp}$ and $\mathbf{v}(n) := \mathbf{R}_{\rm cp}\mathbf{w}(n)$, we obtain after the CP removal the following input-output relationship:

$$\mathbf{y}(n) = e^{j\omega_o(nP+\overline{L})}\mathbf{D}_N(\omega_o)\mathbf{H}\mathbf{F}_N^{\mathcal{H}}\mathbf{T}_{\rm sc}\mathbf{s}(n) + \mathbf{v}(n). \quad (4)$$

It is easily verified that $\mathbf{H}$ is a circulant matrix with $[\mathbf{H}]_{k,l} = h((k-l) \bmod N)$. Recalling that circulant matrices are diagonalized by FFT matrices [6, p. 202], we obtain $\mathbf{F}_N\mathbf{H}\mathbf{F}_N^{\mathcal{H}} = \mathbf{D}_N(\tilde{\mathbf{h}}_N)$, where $\tilde{\mathbf{h}}_N := [\tilde{h}(0)\cdots\tilde{h}(2\pi(N-1)/N)]^T$, with $\tilde{h}(2\pi n/N) := \sum_{l=0}^{L} h(l)\,\exp(-j2\pi \ln/N)$ denoting the channel's frequency response values at the FFT grid. Next, we insert $\mathbf{F}_N^{\mathcal{H}}\mathbf{F}_N = \mathbf{I}_N$ between $\mathbf{D}_N(\omega_o)$ and $\mathbf{H}$ in (4), which does not change the equation. However, using the aforementioned diagonalizing identity of circulant matrices, we can now rewrite (4) as

$$\mathbf{y}(n) = e^{j\omega_o(nP+\overline{L})}\mathbf{D}_N(\omega_o)\mathbf{F}_N^{\mathcal{H}}\mathbf{D}_N(\tilde{\mathbf{h}}_N)\mathbf{T}_{\rm sc}\mathbf{s}(n) + \mathbf{v}(n). \quad (5)$$

Notice from (5) that if the CFO is $\omega_o = 0$ and the noise is absent, then we have $\mathbf{D}_N(\omega_o) = \mathbf{I}_N$ and thus $\mathbf{F}_N\mathbf{y}(n) = \mathbf{D}_N(\tilde{\mathbf{h}}_N)\mathbf{T}_{\rm sc}\mathbf{s}(n)$, confirming that indeed OFDM turns a convolutive channel, represented by $h(l)$, into a multiplicative one, which is captured by the diagonal matrix $\mathbf{D}_N(\tilde{\mathbf{h}}_N)$. In the presence of a CFO, however, since $\mathbf{F}_N\mathbf{D}_N(\omega_o)\mathbf{F}_N^{\mathcal{H}}$ is not diagonal for $\omega_o \neq 0$, the subcarriers are no longer orthogonal and we have *intercarrier interference*, which necessitates the estimation of ω_o and removal of $\mathbf{D}_N(\omega_o)$ from $\mathbf{y}(n)$.

Throughout this paper, we will focus on consistent non-data-aided estimators of ω_o that rely solely on the covariance matrix of $\mathbf{y}(n)$. To express the covariance matrix in a convenient form, we first use the definition of $\mathbf{T}_{\rm sc}$ to verify the identity $\mathbf{D}_N(\tilde{\mathbf{h}}_N)\mathbf{T}_{\rm sc} = \mathbf{T}_{\rm sc}\mathbf{D}_K(\tilde{\mathbf{h}}_K)$, where $[\tilde{\mathbf{h}}_K]_k := \tilde{h}(2\pi\bar{i}_k/N)$, for $k = 1, \ldots, K$. For brevity, we will denote $\tilde{\mathbf{h}} := \tilde{\mathbf{h}}_K$, since we will be primarily working with $\mathbf{D}_K(\tilde{\mathbf{h}}) = \mathbf{D}_K(\tilde{\mathbf{h}}_K)$. We can now express the covariance matrix $\mathbf{R}_{yy} := E[\mathbf{y}(n)\mathbf{y}^{\mathcal{H}}(n)]$ as

$$\mathbf{R}_{yy} = \mathbf{D}_N(\omega_o)\mathbf{F}_N^{\mathcal{H}}\mathbf{T}_{\rm sc}\mathbf{D}_K(\tilde{\mathbf{h}})\mathbf{R}_{ss}\mathbf{D}_K^{\mathcal{H}}(\tilde{\mathbf{h}})\mathbf{T}_{\rm sc}^{\mathcal{H}}\mathbf{F}_N\mathbf{D}_N^{\mathcal{H}}(\omega_o) + \sigma_v^2\mathbf{I}_N \quad (6)$$

where the information symbols $\mathbf{s}(n)$ and the noise $\mathbf{v}(n)$ have covariance matrices $\mathbf{R}_{ss}$ and $\sigma_v^2\mathbf{I}_N$, respectively.

In practice, the ensemble correlation matrix $\mathbf{R}_{yy}$ is replaced by its sample estimate formed by averaging across N_b blocks

$$\hat{\mathbf{R}}_{yy} = \frac{1}{N_b}\sum_{n=0}^{N_b-1}\mathbf{y}(n)\mathbf{y}^{\mathcal{H}}(n). \quad (7)$$

Starting from (5), it is easy to verify that $\hat{\mathbf{R}}_{yy}$ satisfies (6) with sufficiently large N_b, provided that $\mathbf{R}_{ss}$ is replaced by $\hat{\mathbf{R}}_{ss}$, which is defined similar to $\hat{\mathbf{R}}_{yy}$ in (7). Hence, our identifiability results in the ensuing sections apply not only to CFO estimators that are based on $\mathbf{R}_{yy}$ but also to those that rely on $\hat{\mathbf{R}}_{yy}$, provided that N_b is sufficiently large and that the signal-to-noise ratio (SNR) is sufficiently high. In what follows, we will discuss the identifiability of blind CFO estimators that rely on the $\mathbf{R}_{yy}$ of (6), and we will clarify the role of the frequency-selective channel effects in identifiability.

III. Identifiability Issues

Recently, subspace-based CFO estimators have been developed that utilize the covariance matrix $\mathbf{R}_{yy}$ in (6) and assume that the null subcarriers are located at the ends of OFDM blocks [10], [20]. Null subcarriers offer guard bands in the frequency-domain against adjacent channel interference (ACI) and are present in, e.g., the HIPERLAN/2 standard. They can be introduced by zero-padding $\mathbf{s}(n)$ prior to taking the IFFT. Zero-padding can be described by a special zero-inserting matrix $\mathbf{T}_{\rm sc}$ that we define as $\mathbf{T}_{\rm zp} := [\mathbf{I}_K\ \mathbf{0}_{K\times(N-K)}]^T$.

It has been asserted in [10] and [20] that as far as CFO estimation is concerned, one may consider *without loss of generality* (wlog) that the channel is ideal, which in our formulation amounts to having $\mathbf{D}_N(\tilde{\mathbf{h}}_N) = \mathbf{I}_N$. We will show that this wlog assertion does not hold true and that the performance of the CFO estimators in [10], [20] is *channel dependent*. Specifically, we will show that channel zeros on the FFT grid [i.e., zeros on the diagonal of $\mathbf{D}_K(\tilde{\mathbf{h}})$] may cause lack of identifiability of the CFO. Lack of identifiability implies inconsistent CFO estimators; i.e., no matter how many data blocks are used to form sample estimates $\hat{\mathbf{R}}_{yy}$ of $\mathbf{R}_{yy}$, the resulting CFO estimator $\hat{\omega}_0$ is not guaranteed to converge to the true ω_o. In the following theorem (see Appendix A for the proof), we claim that if the null subcarrier insertion matrix $\mathbf{T}_{\rm sc} = \mathbf{T}_{\rm zp}$, as is the case with [10] and [20], then no method that relies on $\mathbf{R}_{yy}$ alone uniquely determines ω_o and $h(l)$.

Theorem 1: For the choice $\mathbf{T}_{\rm sc} = \mathbf{T}_{\rm zp}$, there exist at least two pairs of CFO and channel $(\omega_o, h(l)) \neq (\omega_o', h'(l))$ that give rise to the same $\mathbf{R}_{yy}$ in (6).

Two remarks are now in order.

Remark 1: The fact that symbol correlation matrix $\mathbf{R}_{ss}$ is Toeplitz is instrumental in showing that $\mathbf{R}_{yy}$ does not determine $(\omega_o, h(l))$ uniquely. If $\mathbf{s}(n)$ is linearly precoded with a matrix to obtain $\overline{\mathbf{s}}(n) := \mathbf{C}\mathbf{s}(n)$, *before* the null subcarrier insertion (which would render $\mathbf{R}_{\overline{s}\,\overline{s}}$ non-Toeplitz), then there is a chance that the resulting $\mathbf{R}_{yy}$ determines $(\omega_o, h(l))$ uniquely. This suggests that linearly precoding the information blocks $\mathbf{s}(n)$ might be useful for CFO identifiability based on null subcarriers. However, we will not pursue this interesting research direction herein.

Remark 2: Notice that Theorem 1 makes the claim that *any* method that solely relies on the correlation matrix of received blocks $\mathbf{R}_{yy}$ or its sample estimates in (7) and uses $\mathbf{T}_{\rm sc} = \mathbf{T}_{\rm zp}$ has the potential to yield estimates of ω_o that could be confused by ω_o', in the presence of channel zeros on the FFT grid. In what follows, we will discuss the specific identifiability conditions required to render the inconsistent MUSIC- and ESPRIT-like estimators of [10] and [20] consistent and their performance channel-independent.

A. Uniqueness for MUSIC-Based CFO Estimators

The key observation behind the carrier synchronization method of [10] is that the CFO shifts the *set of information* bearing subcarriers to positions where one would expect the *set of null* subcarriers that are prescribed at the transmitter via the zero-padding matrix $\mathbf{T}_{\rm zp}$. Relying on the orthogonality of these two sets, it is possible to estimate the CFO based on

the null space of $\mathbf{R}_{yy}$ using a MUSIC-like algorithm [10]. Alternatively, one may introduce a cost function that measures this CFO-induced shift; its minimum yields the desired CFO.[1] With our notation, this cost function can be written as a sum of quadratic forms

$$J(\omega) := \sum_{k=1}^{N-K} \mathbf{f}_N^{\mathcal{H}}\left(\frac{2\pi i_k}{N}\right)\mathbf{D}_N^{-1}(\omega)\mathbf{R}_{yy}\mathbf{D}_N(\omega)\mathbf{f}_N\left(\frac{2\pi i_k}{N}\right) \tag{8}$$

where ω is the candidate CFO. Using $\mathbf{T}_{\rm zp}$ instead of $\mathbf{T}_{\rm sc}$, as in [10], we can replace the sum over $\{i_k\}_{k=1}^{N-K}$ in (8) by a sum over $\{K, \ldots, N-1\}$. After substituting (6) into (8), we can reexpress $J(\omega)$ as

$$\begin{aligned} J(\omega) = \sum_{k=K}^{N-1}\Bigg[&\mathbf{f}_N^{\mathcal{H}}\left(\frac{2\pi k}{N}\right)\mathbf{D}_N(\omega_o-\omega)\mathbf{F}_N^{\mathcal{H}}\mathbf{T}_{\rm zp}\mathbf{D}_K(\tilde{\mathbf{h}})\mathbf{R}_{ss} \\ &\cdot\mathbf{D}_K^{\mathcal{H}}(\tilde{\mathbf{h}})\mathbf{T}_{\rm zp}^{\mathcal{H}}\mathbf{F}_N\mathbf{D}_N^{\mathcal{H}}(\omega_o-\omega)\mathbf{f}_N\left(\frac{2\pi k}{N}\right)\Bigg] \\ &+\sigma_v^2\sum_{k=K}^{N-1}\mathbf{f}_N^{\mathcal{H}}\left(\frac{2\pi k}{N}\right)\mathbf{D}_N(\omega)\mathbf{I}_K \\ &\cdot\mathbf{D}_N^{\mathcal{H}}(\omega)\mathbf{f}_N\left(\frac{2\pi k}{N}\right). \end{aligned} \tag{9}$$

The second sum on the right-hand side (RHS) of (9) is due to the AWGN and can be simplified to $(N-K)\sigma_v^2$, which does not depend on ω. Thus, it can be dropped from the cost function that is used for CFO estimation based on the criterion

$$\hat{\omega}_o = \arg\min_{\omega} J(\omega). \tag{10}$$

To understand why minimization of $J(\omega)$ may yield the CFO, note first that $\omega=\omega_o$ implies $\mathbf{D}_N(\omega_o-\omega)=\mathbf{I}_N$ in (9). Next, recall that the matrix $\mathbf{F}_N^{\mathcal{H}}\mathbf{T}_{\rm zp}$ consists of the first K columns of $\mathbf{F}_N^{\mathcal{H}}$ that are orthogonal to $\{\mathbf{f}_N(2\pi k/N)\}_{k=K}^{N-1}$. Hence, if $\omega=\omega_o$, the quadratic forms in the first sum of (9) are zero and $J(\omega_o)\equiv(N-K)\sigma_v^2$ in the presence of noise (or $J(\omega_o)\equiv 0$ in the absence of noise).

The zeros of $J(\omega)$ have been claimed in [10] to yield the CFO in the absence of noise. We have confirmed that ω_o is indeed a zero of $J(\omega)$ in the absence of noise. However, whether ω_o is the *only* zero of $J(\omega)$ has to be established as well before validating (10) for CFO estimation, which is an issue that has not been addressed in [10]. In fact, ω_o will turn out to be the unique zero (or the only minimum) of $J(\omega)$ under conditions that guarantee $\mathbf{D}_K(\tilde{\mathbf{h}})$ is full rank. To see this, recall that $J(\omega)$ in (9) is a sum of nonnegative quadratic forms that are zero if and only if

$$\mathbf{f}_N^{\mathcal{H}}\left(\frac{2\pi k}{N}+\omega_o-\omega\right)\mathbf{F}_N^{\mathcal{H}}\mathbf{T}_{\rm zp}\mathbf{D}_K(\tilde{\mathbf{h}})=\mathbf{0},\quad \forall k\in[K,\,N-1]. \tag{11}$$

If $\mathbf{D}_K(\tilde{\mathbf{h}})$ is full rank, then (11) is equivalent to $\mathbf{f}_N^{\mathcal{H}}(2\pi k/N+\omega_o-\omega)\mathbf{F}_N^{\mathcal{H}}\mathbf{T}_{\rm zp}=\mathbf{0}$, $\forall k\in[K,N-1]$. Clearly the left nullspace of $\mathbf{F}_N^{\mathcal{H}}\mathbf{T}_{\rm zp}$ has dimensionality $N-K$. Because $\mathbf{f}_N^{\mathcal{H}}(2\pi k/N+\omega_o-\omega)$ is a Vandermonde vector[2] and since the only Vandermonde vectors that are in the left null space of $\mathbf{F}_N^{\mathcal{H}}\mathbf{T}_{\rm zp}$ are $\{\mathbf{f}_N^{\mathcal{H}}(2\pi k/N)\}_{k=K}^{N-1}$, it follows that $\{\mathbf{f}_N^{\mathcal{H}}(2\pi k/N)\}_{k=K}^{N-1}=\{\mathbf{f}_N^{\mathcal{H}}(2\pi k/N+\omega_o-\omega)\}_{k=K}^{N-1}$. But this is only possible whenever $\{2\pi k/N\}_{k=K}^{N-1}=\{2\pi k/N+\omega_o-\omega\}_{k=K}^{N-1}$, which is the case if and only if $\omega_o=\omega \bmod 2\pi$.

In the previous discussion, we proved that for $J(\omega)$ to have a unique minimum, it is sufficient for $\mathbf{D}_K(\tilde{\mathbf{h}})$ to be full rank. However, this condition is not necessary. The necessary and sufficient conditions for $J(\omega)$ to have a unique minimum are given in the following theorem.

Theorem 2: Suppose that $N-K>L$ and $\mathbf{T}_{\rm sc}=\mathbf{T}_{\rm zp}$. Then, for $J(\omega)$ to have a unique minimum, it is necessary and sufficient that both $\tilde{h}(0)\neq 0$ and $\tilde{h}(2\pi(K-1)/N)\neq 0$ hold.

Proof: We have already established that $J(\omega)$ is minimized if and only if (11) holds. Let $\{2\pi\kappa_i/N\}_{i=1}^{I}$ denote the set of channel zeros on the FFT grid [i.e., the κ_is satisfy $\tilde{h}(2\pi\kappa_i/N)=0$, for $i=1,\ldots,I\le L$]. Then, (11) holds if and only if $\{\mathbf{f}_N(2\pi k/N+\omega_o-\omega\}_{k=K}^{N-1}$ is in the left null space (LNS) of $\mathbf{F}_N^{\mathcal{H}}\mathbf{T}_{\rm zp}\mathbf{D}_K(\tilde{\mathbf{h}})$. The LNS of $\mathbf{T}_{\rm zp}\mathbf{D}_K(\tilde{\mathbf{h}})$ is given by $\{\mathbf{e}_k\}_{k=K}^{N-1}\cup\{\mathbf{e}_{\kappa_i}\}_{i=1}^{I}$. Therefore, using the orthogonality of $\mathbf{F}_N^{\mathcal{H}}$, the LNS of $\mathbf{F}_N^{\mathcal{H}}\mathbf{T}_{\rm zp}\mathbf{D}_K(\tilde{\mathbf{h}})$ can be seen to be $\{\mathbf{f}_N(2\pi k/N)\}_{k=K}^{N-1}\cup\{\mathbf{f}_N(2\pi\kappa_i/N)\}_{i=1}^{I}$. In other words, (11) holds if and only if

$$\left\{\frac{2\pi k}{N}+\omega-\omega_o\right\}_{k=K}^{N-1}\subset\left(\left\{\frac{2\pi k}{N}\right\}_{k=K}^{N-1}\cup\left\{\frac{2\pi\kappa_i}{N}\right\}_{i=1}^{I}\right). \tag{12}$$

Equation (12) clearly holds for $\omega=\omega_o$. To find the conditions for the existence of other zeros of $J(\omega)$, notice that (12) holds for $\omega\neq\omega_o$ if and only if the union $\{K,\ldots,N-1\}\cup\{\kappa_i\}_{i=1}^{I}$ contains $N-K$ consecutive elements that are not all taken from the set $\{K,\ldots,N-1\}$. Because $I\le L$ and the channel has $L<N-K$ zeros, the set of $N-K$ consecutive elements must have some elements from $\{K,\ldots,N-1\}$ in it. But this is possible if and only if $0\in\{\kappa_i\}_{i=1}^{I}$, or $K-1\in\{\kappa_i\}_{i=1}^{I}$. In other words, we have established that $\{\tilde{h}(0)\neq 0$ and $\tilde{h}(2\pi(K-1)/N)\neq 0\}$ if and only if $J(\omega)$ has a unique solution. ■

The implication of Theorem 2 is that carrier synchronization based on *consecutive* null subcarriers is *channel dependent*, unlike what is stated in [10]. Notice that the "consecutive" spacing should be understood in a circular sense, where the first (zeroth) subcarrier is considered adjacent to the last $(N-1)$st one. Because the channel is neither known nor fixed, when selecting consecutive null subcarriers, one has no means of assuring identifiability and channel-independent performance with the CFO estimators in [10]. Having recognized the problem, we will proceed to alter the consecutive null subcarrier transmission strategy in the next section.

But at this point, one may wonder how likely it is for $\mathbf{D}_K(\tilde{\mathbf{h}})$ to be rank-deficient and what the effect of (near) rank deficiency in the overall system performance may be. Even when $\mathbf{D}_K(\tilde{\mathbf{h}})$

[1]Viewing this cost function as measuring the energy falling into the subbands corresponding to the set of null subcarriers, [1] used $J(\omega)$ to derive adaptive CFO estimation algorithms (see also Section V).

[2]Vandermonde $N\times 1$ vectors $\{\mathbf{v}_N(g_i)\}_{i=1}^{T}$ with generators $\{g_i\}$ have the form $\mathbf{v}_N(g_i):=[1,\,g_i,\,\ldots,\,g_i^{N-1}]^T$ and they are linearly independent so long as their generators are distinct; i.e., $g_i\neq g_k$ for $i\neq k$.

has full rank, if its diagonal entries have small values, the performance of the CFO estimator will suffer considerably. In other words, the event of having channel zeros on the FFT grid may have measure zero, but having channel zeros within a neighborhood close to the FFT grid is likely. And as our simulations will confirm, the effect of such zeros in CFO estimation and symbol recovery is important. This is also the case for the ESPRIT-based approach in [20], which we discuss next.

B. Uniqueness for ESPRIT-Based CFO Estimators

ESPRIT is a high-resolution technique for frequency estimation that has been invoked by [20] to find a closed-form expression for ω_o in terms of the singular vectors of $\mathbf{R}_{yy}$. We will briefly develop the general ESPRIT algorithm and then delineate how it was used in [20] for CFO estimation before we develop our identifiability results.

Consider the following parameterization of the $N \times N$ covariance matrix of p sinusoids with frequencies $\theta_1, \ldots, \theta_p$ in noise (see [19] for a detailed discussion):

$$\mathbf{R} = \mathbf{A}\mathbf{P}\mathbf{A}^{\mathcal{H}} + \sigma_v^2\mathbf{I}_N \tag{13}$$

where $\mathbf{A} := [\mathbf{f}_N(\theta_1)\cdots\mathbf{f}_N(\theta_p)]$ and $\mathbf{P}$ is an $N \times N$ full-rank mixing matrix, which, in the conventional frequency estimation problem, is a diagonal matrix with the amplitudes of the sinusoids on its diagonal. Let $\mathbf{R} = [\mathbf{S},\ \mathbf{G}]\mathbf{D}[\mathbf{S},\ \mathbf{G}]^{\mathcal{H}}$ be the singular value decomposition (SVD) of $\mathbf{R}$ so that the range space $\mathcal{R}(\mathbf{S}) = \mathcal{R}(\mathbf{R})$. Define also $\mathbf{S}_1 := [\mathbf{I}_{N-1}\ \ \mathbf{0}]\mathbf{S}$ and $\mathbf{S}_2 := [\mathbf{0}\ \ \mathbf{I}_{N-1}]\mathbf{S}$. Then, it can be shown that the eigenvalues of $\mathbf{\Phi} := (\mathbf{S}_1^{\mathcal{H}}\mathbf{S}_1)^{-1}\mathbf{S}_1^{\mathcal{H}}\mathbf{S}_2$ are given by $\exp(-j\theta_1), \ldots, \exp(-j\theta_p)$, from which the desired $\theta_1 \cdots \theta_p$ can be obtained. Note that the estimate of $\mathbf{R}$ in (7) can be used to obtain an estimate of $\mathbf{\Phi}$ whose eigenvalues determine the frequencies of interest.

To understand how the ESPRIT algorithm can be used in estimating the CFO, one should note that (6) is in the same form as (13) with $p = K$, $\mathbf{P} = \mathbf{D}_K(\tilde{\mathbf{h}})\ \mathbf{R}_{ss}\ \mathbf{D}_K^{\mathcal{H}}(\tilde{\mathbf{h}})$, $\mathbf{A} = \mathbf{D}_N(\omega_o)\mathbf{F}_N^{\mathcal{H}}\mathbf{T}_{\rm sc}$, and $\theta_k = 2\pi(k-1)/N + \omega_o$. Since the ESPRIT algorithm yields a matrix $\mathbf{\Phi}$ whose eigenvalues are complex exponential with phases given by $-\theta_i$, applying ESPRIT to $\mathbf{R}_{yy}$ will yield a $\mathbf{\Phi}$ whose trace (sum of the diagonal elements, which is equal to sum of the eigenvalues) will be given by $\mathrm{tr}(\mathbf{\Phi}) = \sum_{k=1}^{K}\exp(-j\theta_k) = \exp(-j\omega_o)\sum_{k=1}^{K}\exp(-j2\pi(k-1)/N)$. From the latter, we can obtain the CFO in closed form as [20]

$$\omega_o = -\arg\left(\frac{\mathrm{tr}(\mathbf{\Phi})}{\sum_{k=1}^{K}\exp(-j2\pi(k-1)/N)}\right).$$

Even though this application of ESPRIT yields an elegant closed-form expression for ω_o, it also suffers from identifiability problems, similar to the MUSIC-like algorithm of the SectionIII-A. The reason is that the ESPRIT algorithm requires $\mathbf{P}$ to be full rank, which for our problem might not be the case if $\mathbf{D}_K(\tilde{\mathbf{h}})\ \mathbf{R}_{ss}\ \mathbf{D}_K^{\mathcal{H}}(\tilde{\mathbf{h}})$ loses rank due to channel nulls on the FFT grid. Moreover, unlike the minimization of the cost function in (8), ESPRIT requires taking the SVD of $\mathbf{R}_{yy}$, which is computationally complex.

It was shown in [19] that the asymptotic variance of ESPRIT-based frequency estimators increases whenever the mixing matrix $\mathbf{P}$ of (13), or correspondingly the matrix $\mathbf{D}_K(\tilde{\mathbf{h}})\mathbf{R}_{ss}\mathbf{D}_K^{\mathcal{H}}(\tilde{\mathbf{h}})$ of (6) for our problem, becomes ill-conditioned. This suggests that channel zeros on or close to the unit circle will adversely affect the performance of the ESPRIT-based frequency estimation algorithm in [20].

In what follows, we will introduce remedies to the loss of identifiability and performance by altering the placement of null subcarriers that were padded at the ends of OFDM blocks in [10] and [20]. Our first remedy will place null subcarriers in a special way, while our second remedy will be to randomly hop their locations from block to block. Both approaches will assure channel-independent identifiability.

IV. Consistent CFO Estimators

After realizing that channel zeros may cause loss of identifiability, as discussed in the last section, the natural question that arises is how the null subcarriers should be placed in order to restore identifiability. One way of doing this is to adjust the spacing of the null carriers in a special way, in order to guarantee a unique minimum for $J(\omega)$ regardless of the underlying frequency-selective channel. Another alternative is to "hop" the null carriers from block to block, which amounts to making $\mathbf{T}_{\rm sc}$ dependent on the block index n. We will discuss the former option first.

A. Null Subcarriers With Distinct Spacings

In the following theorem, we establish that even in the presence of up to L channel zeros on the FFT grid, judicious spacing of the null subcarriers guarantees a unique minimum for $J(\omega)$ in (8).

Theorem 3: Let $i_k,\ k = 1, \ldots, N-K$ denote the indexes of the null subcarriers with frequencies $2\pi i_k/N$ and let i_k be chosen so that $i_{k_1} - i_{k_2} = i_{k_3} - i_{k_4} \Rightarrow k_1 = k_3$ and $k_2 = k_4$ (i.e., with all possible spacings being distinct). If we choose the number of null subcarriers to be $N - K = L + 2$, with the spacing condition indicated above, then (8) has a unique solution given by $\omega = \omega_o$, regardless of where the L zeros of the channel are located.

Proof: As was mentioned before, the values of ω that attain the minima of $J(\omega)$ when $\sigma_v^2 > 0$ coincide with the zeros of $J(\omega)$ when $\sigma_v^2 = 0$. So, without loss of generality, we will assume that $\sigma_v^2 = 0$ and show that $J(\omega) = 0$ implies that $\omega = \omega_o \bmod 2\pi$.

Since every term in (8) is nonnegative, $J(\omega) = 0$ if and only if

$$\mathbf{f}_N^{\mathcal{H}}\left(\frac{2\pi i_k}{N}\right)\mathbf{D}_N^{-1}(\omega)\mathbf{R}_{yy}\mathbf{D}_N(\omega)\mathbf{f}_N\left(\frac{2\pi i_k}{N}\right) = 0, \quad \forall k \in [1,\ L+2]. \tag{14}$$

Using (6), it follows that (14) is equivalent to

$$\mathbf{f}_N^{\mathcal{H}}\left(\frac{2\pi i_k}{N}\right)\mathbf{D}_N^{-1}(\omega-\omega_o)\mathbf{F}_N^{\mathcal{H}}\mathbf{T}_{\rm sc}\mathbf{D}_K(\tilde{\mathbf{h}}) = 0, \quad \forall k \in [1,\ L+2]. \tag{15}$$

Suppose that the channel has $I \leq L$ zeros on the FFT grid at frequencies $\mathcal{K}_o := \{2\pi\kappa_i/N\}_{i=1}^{I}$, and let $\mathcal{K}_{\rm sc} := \{2\pi i_k/N\}_{k=1}^{L+2}$ denote the set of null subcarrier frequencies. Similar to the argument that follows (11), (15) is satisfied if and only if $\mathbf{f}_N^{\mathcal{H}}(2\pi i_k/N)\mathbf{D}_N^{-1}(\omega - \omega_o) = \mathbf{f}_N^{\mathcal{H}}(2\pi i_k/N + \omega - \omega_o)$ is in the left null space of $\mathbf{F}_N^{\mathcal{H}}\mathbf{T}_{\rm sc}\mathbf{D}_K(\tilde{\mathbf{h}})$. An orthonormal basis for the left null space of $\mathbf{F}_N^{\mathcal{H}}\mathbf{T}_{\rm sc}\mathbf{D}_K(\tilde{\mathbf{h}})$ is given by $\mathcal{F} := \mathcal{F}_{\rm sc} \cup \mathcal{F}_o$, where $\mathcal{F}_{\rm sc} := \{\mathbf{f}_N^{\mathcal{H}}(2\pi i_k/N)\}_{k=1}^{L+2}$ and $\mathcal{F}_o := \{\mathbf{f}_N^{\mathcal{H}}(2\pi\kappa_i/N)\}_{i=1}^{I}$. Therefore, (15) holds if and only if

$$\mathbf{f}_N^{\mathcal{H}}\left(\frac{2\pi i_k}{N} + \omega - \omega_o\right) \in \text{span}(\mathcal{F}), \qquad \forall k \in [1,\, L+2]. \tag{16}$$

Because $\{\mathbf{f}_N^{\mathcal{H}}(2\pi i_k/N + \omega - \omega_o)\}_{k=1}^{L+2}$ are Vandermonde vectors, and since the only Vandermonde vectors in span($\mathcal{F}$) are also in $\mathcal{F}$, it follows that $\mathbf{f}_N^{\mathcal{H}}(2\pi i_k/N + \omega - \omega_o) \in \mathcal{F}$, $\forall k \in [1, L+2]$. This in turn implies that $\mathbf{f}_N^{\mathcal{H}}(2\pi i_k/N + \omega - \omega_o) \in \mathcal{F}_{\rm sc} \cup \mathcal{F}_o$, $\forall k \in [1, L+2]$, which is equivalent to

$$\frac{2\pi i_k}{N} + \omega - \omega_o \in \mathcal{K}_{\rm sc} \cup \mathcal{K}_o, \qquad \forall k \in [1, L+2]. \tag{17}$$

Because the number of elements in $\mathcal{K}_o$ is no greater than L, at least two elements of the $(L+2)$-element set $\{2\pi i_k/N + \omega - \omega_o\}_{k=1}^{L+2}$ must belong to $\mathcal{K}_{\rm sc}$. Let these two elements be denoted by $\omega_1 := 2\pi i_{k_1}/N + \omega - \omega_o$ and $\omega_2 := 2\pi i_{k_2}/N + \omega - \omega_o$. But since $\omega_1, \omega_2, 2\pi i_{k_1}/N, 2\pi i_{k_2}/N \in \mathcal{K}_{\rm sc}$, we have that $\omega_1 - \omega_2 = 2\pi i_{k_1}/N - 2\pi i_{k_2}/N \Rightarrow \omega_1 = 2\pi i_{k_1}/N$ due to the condition of "distinct spacings" assumed by the theorem. But since $\omega_1 := 2\pi i_{k_1}/N + \omega - \omega_o = 2\pi i_{k_1}/N$, we have that $\omega - \omega_o = 0 \bmod 2\pi$, which is precisely what we wanted to prove. ∎

The algorithms in [10] and [20] do not assure channel-independent performance, but also they do not specify the number of null subcarriers required for unique CFO estimation. In addition to providing a means to preserve identifiability, Theorem 3 shows that by proper spacing of the null subcarriers, the number of subcarriers needed to make $J(\omega)$ have a unique minimum is $L+2$, i.e., on the order of L, *regardless of the channel zero locations*. Notice that selecting (N, K) to satisfy $N - K \geq L + 2$ and $N \geq 2^{N-K}$, the simple choice of $i_k = 2^{k-1}$, $k = 1, \ldots, N - K$ satisfies the condition of "distinct spacings" in Theorem 3. In what follows, we provide an alternative approach to guarantee channel-independent identifiability by "hopping" the null carriers from block to block.

B. Null Subcarrier Hopping

The idea behind null subcarrier hopping is to make $\mathbf{T}_{\rm sc}$ dependent on the block index n, with the hopping pattern known to both the transmitter and the receiver. Null subcarrier hopping was originally suggested in [1], where CFO estimators for *multiuser* OFDM transmissions were developed as well. The novelty of the present derivation for *single-user* OFDM systems is twofold: null subcarrier hopping is derived here using the matrix-vector formulation. Unlike [1], which uses a deterministic hopping condition, here the proof relies on the randomness of the hopping pattern.

We will select the length of information blocks $K > L$ and suppose that for each block, the null carriers are consecutive, but their locations are randomly chosen. To this end, we will invoke a random variable q_n that is uniformly distributed on $\{1, \ldots, N\}$ and that determines the location of the consecutive null subcarriers whose value is known to both the transmitter and the receiver. The corresponding $N \times K$ null subcarrier insertion matrix will now depend on the block index n as

$$\mathbf{T}_{\rm sc}(n) := \left[\mathbf{e}_{q_n (\bmod N)}\, \mathbf{e}_{q_n+1 (\bmod N)} \cdots \mathbf{e}_{q_n+K-1 (\bmod N)}\right]$$

so that [see (5)]

$$\mathbf{y}(n) = e^{j\omega_o(nP+\overline{L})}\mathbf{D}_N(\omega_o)\mathbf{F}_N^{\mathcal{H}}\mathbf{D}_N(\tilde{\mathbf{h}}_N)\mathbf{T}_{\rm sc}(n)\mathbf{s}(n) + \mathbf{v}(n).$$

Substituting directly from the definitions of $\mathbf{T}_{\rm sc}(n)$ and $\mathbf{D}(\tilde{\mathbf{h}})$, it follows that $\mathbf{D}_N(\tilde{\mathbf{h}}_N)\mathbf{T}_{\rm sc}(n) = \mathbf{T}_{\rm sc}(n)\mathbf{D}_K(\tilde{\mathbf{h}}_K(q_n))$, where $\tilde{\mathbf{h}}_K(q_n) = [\tilde{h}(2\pi q_n/N), \tilde{h}(2\pi(q_n+1)/N), \ldots, \tilde{h}(2\pi(q_n + K-1)/N)]^T$. For convenience, let us define the "unhop matrix" $\mathbf{D}_N^{\mathcal{H}}(2\pi q_n/N)$. Operating on the received blocks with the "unhop matrix," we obtain

$$\begin{aligned}\overline{\mathbf{y}}(n)\theta s :=& \mathbf{D}_N^{\mathcal{H}}\left(\frac{2\pi q_n}{N}\right)\mathbf{y}(n)\\ =& e^{j\omega_o(nP+\overline{L})}\mathbf{D}_N(\omega_o)\mathbf{D}_N^{\mathcal{H}}\left(\frac{2\pi q_n}{N}\right)\mathbf{F}_N^{\mathcal{H}}\mathbf{T}_{\rm sc}(n)\\ &\cdot \mathbf{D}_K(\tilde{\mathbf{h}}_K(q_n))\mathbf{s}(n) + \mathbf{D}_N^{\mathcal{H}}\left(\frac{2\pi q_n}{N}\right)\mathbf{v}(n).\end{aligned} \tag{18}$$

The crucial point to realize here is that $\mathbf{D}_N^{\mathcal{H}}(2\pi q_n/N)\mathbf{F}_N^{\mathcal{H}}\mathbf{T}_{\rm sc}(n) = \mathbf{F}_N^{\mathcal{H}}\mathbf{T}_{\rm zp}$, which consists of the first K columns of $\mathbf{F}_N^{\mathcal{H}}$ and is *independent* of n. The autocorrelation matrix of $\overline{\mathbf{y}}(n)$ in (18) is thus

$$\begin{aligned}\mathbf{R}_{\overline{y}\,\overline{y}} = \mathbf{D}_N(\omega_o)\mathbf{F}_N^{\mathcal{H}}\mathbf{T}_{\rm zp}E\left[\mathbf{D}_K(\tilde{\mathbf{h}}_K(q_n))\mathbf{R}_{ss}\mathbf{D}_K^{\mathcal{H}}(\tilde{\mathbf{h}}_K(q_n))\right]\\ \cdot\mathbf{T}_{\rm zp}^{\mathcal{H}}\mathbf{F}_N\mathbf{D}_N^{\mathcal{H}}(\omega_o) + \sigma_v^2\mathbf{I}_N\end{aligned} \tag{19}$$

where the expectation is with respect to q_n after making use of the fact that $s(n)$ is independent of q_n. Because q_n is uniformly distributed, it follows that

$$\begin{aligned}E\left[\mathbf{D}_K(\tilde{\mathbf{h}}_K(q_n))\mathbf{R}_{ss}\mathbf{D}_K^{\mathcal{H}}(\tilde{\mathbf{h}}_K(q_n))\right]\\ = \frac{1}{N}\sum_{m=0}^{N-1}\mathbf{D}_K(\tilde{\mathbf{h}}_K(m))\mathbf{R}_{ss}\mathbf{D}_K^{\mathcal{H}}(\tilde{\mathbf{h}}_K(m)).\end{aligned} \tag{20}$$

We maintain that the expectation in (20) is a positive definite (and hence full rank) matrix. To see this, consider the following quadratic form: $\mathbf{z}^{\mathcal{H}}[N^{-1}\sum_{m=0}^{N-1}\mathbf{D}_K(\tilde{\mathbf{h}}_K(m))\mathbf{R}_{ss}\mathbf{D}_K^{\mathcal{H}}(\tilde{\mathbf{h}}_K(m))]\mathbf{z}$. For the latter to be zero, we must have $\mathbf{z}^{\mathcal{H}}\mathbf{D}_K(\tilde{\mathbf{h}}_K(m))\mathbf{R}_{ss}\mathbf{D}_K^{\mathcal{H}}(\tilde{\mathbf{h}}_K(m))\mathbf{z} = \mathbf{0}$, $\forall m \in [0, N-1]$. Because $\mathbf{R}_{ss}$ is full rank, we infer that $\mathbf{z}^{\mathcal{H}}\mathbf{D}_K(\tilde{\mathbf{h}}_K(m)) = 0$, $\forall m \in [0, N-1]$. But $\mathbf{D}_K(\tilde{\mathbf{h}}_K(m))$ can have at most L zeros on its diagonal, and we have chosen $K > L$; hence, we have that $\mathbf{z} = \mathbf{0}$, which shows that (20) is full rank. Notice that if $\mathbf{R}_{ss} = \sigma_s^2\mathbf{I}_K$, then (20) becomes

$$\begin{aligned}\sigma_s^2 E\left[\mathbf{D}_K(\tilde{\mathbf{h}}_K(q_n))\mathbf{D}_K^{\mathcal{H}}(\tilde{\mathbf{h}}_K(q_n))\right]\\ = \sigma_s^2 N^{-1}\sum_{m=0}^{N-1}\left|\tilde{h}(2\pi m/N)\right|^2\mathbf{I}_K\end{aligned}$$

which is clearly seen to be full rank.

We established that the rank of the covariance matrix of the received block $\overline{\mathbf{y}}(n)$ after "unhopping" is independent of the channel zero locations, due to the block-by-block averaging in-

duced by null subcarrier hopping, regardless of the color of the input symbols. Using $\mathbf{R}_{\overline{y}\,\overline{y}}$ instead of $\mathbf{R}_{yy}$ for the MUSIC-based CFO estimator in (9) and (10) guarantees that the resulting cost function $J(\omega)$ will have a unique minimum. Likewise, if $\mathbf{R}_{\overline{y}\,\overline{y}}$ is used in the ESPRIT algorithm, the mixing matrix $\mathbf{P}$ in (13) will be given by (20), which is always full rank, and hence the algorithm will not suffer from channel fades.

Relying on a *deterministic* hopping pattern, it was shown in [1] that the cost function is also independent of the channel zero locations when the input symbols are uncorrelated. Here, we exploit our matrix-vector model to generalize this result to correlated symbols ($\mathbf{R}_{ss} \neq \sigma_s^2\mathbf{I}_K$). In addition, we use a pseudo *random* hopping pattern, which avoids the need to choose the number of available received blocks to be a multiple of N. Moreover, combining the channel-independent aspect of the null subcarrier hopping with our results from Section III-A, we not only assure performance independent of channel zeros but also establish that hopping guarantees a unique minimum for $J(\omega)$.

C. Combining Hopping With Consecutive Null Subcarriers

In both the HIPERLAN/2 and the IEEE802.11a standards, null subcarriers are padded to each block in order to suppress ACI [5], [7]. In Section IV-B, we established that hopping can guarantee CFO identifiability. Thus, it is natural to ask whether these two methods can be combined. In this section, we will propose a method that benefits from both hopping and null subcarrier padding.

This hybrid method proceeds in two steps for null subcarrier insertion. First, we pad $N-K-1$ zeros to each block $\mathbf{s}(n)$ using $\overline{\mathbf{T}}_{\rm zp} := [\mathbf{I}_K\ \mathbf{0}_{K\times(N-K-1)}]^T$. Then, we randomly insert another null subcarrier by left multiplying $\mathbf{T}_{\rm zp}\mathbf{s}(n)$ with $\mathbf{T}_{\rm sc}(n) = [\mathbf{e}_{q_n(\mathrm{mod}\,N)}, \ldots, \mathbf{e}_{q_n+N-2(\mathrm{mod}\,N)}]$. Note that $\mathbf{T}_{\rm sc}(n)$ here is an $N\times(N-1)$ matrix; i.e., only one null subcarrier is hopping. Thus, $N-K$ null subcarriers have been separated into two classes: one class with size $N-K-1$ is padded at the end of each block, and another one is hopping from block to block within locations $[0,\ N-1]$. Equation (5) now becomes

$$\mathbf{y}(n) = e^{j\omega_o(nP+\overline{L})}\mathbf{D}_N(\omega_o)\mathbf{F}_N^{\mathcal{H}}\mathbf{D}_N(\tilde{\mathbf{h}}_N)\mathbf{T}_{\rm sc}(n) \cdot \overline{\mathbf{T}}_{\rm zp}\mathbf{s}(n) + \mathbf{v}(n).$$

Similar to Section IV-B, we know that $\mathbf{D}_N(\tilde{\mathbf{h}}_N)\mathbf{T}_{\rm sc}(n) = \mathbf{T}_{\rm sc}(n)\mathbf{D}_{N-1}(\tilde{\mathbf{h}}_{N-1}(q_n))$. After "unhopping" the received blocks with the "unhop matrix" $\mathbf{D}_N^{\mathcal{H}}(2\pi q_n/N)$, we obtain

$$\overline{\mathbf{y}}(n) = e^{j\omega_o(nP+\overline{L})}\mathbf{D}_N(\omega_o)\mathbf{D}_N^{\mathcal{H}}(2\pi q_n/N)\mathbf{F}_N^{\mathcal{H}}\mathbf{D}_N(\tilde{\mathbf{h}}_N) \cdot \mathbf{T}_{\rm sc}(n)\overline{\mathbf{T}}_{\rm zp}\mathbf{s}(n) + \mathbf{D}_N^{\mathcal{H}}(2\pi q_n/N)\mathbf{v}(n). \quad (21)$$

Based on the facts that $\mathbf{D}_N^{\mathcal{H}}(2\pi q_n/N)\mathbf{F}_N^{\mathcal{H}}\mathbf{T}_{\rm sc}(n) = \mathbf{F}_N^{\mathcal{H}}[\mathbf{I}_{N-1}\ \mathbf{0}_{(N-1)\times 1}]^T$ and $[\mathbf{I}_{N-1}\ \mathbf{0}_{(N-1)\times 1}]^T\overline{\mathbf{T}}_{\rm zp} = \mathbf{T}_{\rm zp}$, we can simplify (21) as

$$\overline{\mathbf{y}}(n) = e^{j\omega_o(nP+\overline{L})}\mathbf{D}_N(\omega_o)\mathbf{F}_N^{\mathcal{H}}\mathbf{T}_{\rm zp}\mathbf{D}_K(\tilde{\mathbf{h}}_K(q_n))\mathbf{s}(n) + \mathbf{D}_N^{\mathcal{H}}(2\pi q_n/N)\mathbf{v}(n) \quad (22)$$

where $\tilde{\mathbf{h}}_K(q_n) = [\tilde{h}(2\pi q_n/N), \ldots, \tilde{h}(2\pi(q_n+K-1)/N)]^T$. Because $\overline{\mathbf{y}}(n)$ in (21) coincides with $\overline{\mathbf{y}}(n)$ in (18), so do the corresponding autocorrelation matrices. Therefore, all the results and statements in Section IV-B hold true for this new hybrid method.

Comparing the three methods discussed in Section IV-A–C, we deduce that all of them guarantee the identifiability of CFO. However, each has its own advantages. Identifiability for the "distinct spacings" method of Theorem 3 depends on the number and the locations of the null subcarriers, while for the "hopping" methods (Sections IV-B and -C), the identifiability is gained from random subcarrier hopping, so it does not depend on the number and the locations of null subcarriers (without considering channel estimation, $N-K \geq 1$ would have been enough). Recall that our "hopping" methods rely on the statistical averaging over the hopping factor. Under the "distinct spacings" condition and with the same number of data blocks, the method in Section IV-A is thus expected to achieve better performance than that in Section IV-B and -C. The "combination" method in Section IV-C was motivated by the presence of ACI guards in existing standards, though its performance is the same as that of the "pure hopping" method. We will elaborate further on these points in the simulations in Section VI. We close this section with the following remark.

Remark 3: Note that one might also be tempted to rely on pilot carriers, usually invoked for channel estimation, to estimate the CFO. However, pilot tones can be used for CFO estimation when the channel is known. Conversely, pilot-assisted channel estimation requires knowledge of the CFO. Hence, to use nonzero known pilots to estimate the CFO, one needs to know the channel, and vice versa. Null subcarriers can be thought of as zero pilots that enable CFO estimation without the channel knowledge because they nullify the channel effect. We should also point out that usage of null subcarriers does not preclude us from performing non-data-aided channel estimation, for example, with the scheme proposed in [23], after the removal of the CFO.

V. Adaptive CFO Estimators

As we mentioned earlier, the ESPRIT algorithm discussed in Section III-B requires an SVD that is computationally expensive. Finding the minimum of $J(\omega)$, which is the criterion of the MUSIC-like algorithm, also requires a computationally complex exhaustive search for the value of ω that minimizes $J(\omega)$. To avoid this search, [1] suggested that one can alternatively minimize $J(\omega)$ using the following standard gradient algorithm:

$$\hat{\omega}_{o,\,m+1} = \hat{\omega}_{o,\,m} - \mu\left.\frac{\partial J(\omega)}{\partial\omega}\right|_{\omega=\hat{\omega}_{o,\,m}} \quad (23)$$

where $\hat{\omega}_{o,m}$ is the estimate of ω_o at the mth iteration and μ is a stepsize parameter that should be chosen to balance the conflicting requirements of tracking ability and steady-state convergence. To adopt and test (23) for our "distinct spacings," "random hopping," and "combination" methods, we calculate $\partial J(\omega)/\partial\omega$ using the identity

$\mathbf{D}_N(\omega)\mathbf{f}_N(2\pi i_k/N) = \mathbf{D}_N(2\pi i_k/N)\mathbf{f}_N(\omega)$ in (8). We then obtain the following alternative expression for our cost function:

$$J(\omega) = \mathbf{f}_N^{\mathcal{H}}(\omega)\left[\sum_{k=1}^{N-K} \mathbf{D}_N^{\mathcal{H}}\left(\frac{2\pi i_k}{N}\right)\mathbf{R}_{yy}\mathbf{D}_N\left(\frac{2\pi i_k}{N}\right)\right]\mathbf{f}_N(\omega). \tag{24}$$

Using (24), the derivative in (23) can be computed as

$$\frac{\partial J(\omega)}{\partial \omega} = 2\Re\left\{ j\mathbf{f}_N^{\mathcal{H}}(\omega)\left[\sum_{k=1}^{N-K} \mathbf{D}_N^{\mathcal{H}}\left(\frac{2\pi i_k}{N}\right)\mathbf{R}_{yy}\mathbf{D}_N\left(\frac{2\pi i_k}{N}\right) \cdot\mathbf{D}_N(0\colon N-1)\right]\mathbf{f}_N(\omega)\right\} \tag{25}$$

where $\mathbf{D}(0\colon N-1)$ denotes a diagonal matrix with diagonal entries $0, 1, \ldots, N-1$. So, given $\mathbf{R}_{yy}$ or its sample average estimate $\hat{\mathbf{R}}_{yy}$ in (7), one can use (23) and (25) to minimize $J(\omega)$ iteratively.

To apply the gradient algorithm (23) online, we must express each time update $\omega_o(n+1)$ in terms of the incoming data $\mathbf{y}(n)$. Toward this objective, we use the standard recursion to update our covariance matrix estimates at time n: $\hat{\mathbf{R}}_{yy}(n) = \alpha\hat{\mathbf{R}}_{yy}(n-1) + (1-\alpha)\mathbf{y}(n)\mathbf{y}^{\mathcal{H}}(n)$, where $0 \le \alpha < 1$ is a parameter that can be adjusted depending on the variation of the CFO. The adaptive algorithm then becomes

$$\hat{\omega}_o(n+1) = \hat{\omega}_o(n) - \mu\left.\frac{\partial J(\omega)}{\partial \omega}\right|_{\omega=\hat{\omega}_o(n)} \tag{26}$$

where the derivative of the cost function is computed as in (25) but with $\mathbf{R}_{yy}$ replaced by

$$\hat{\mathbf{R}}_{yy}(n) = \alpha\hat{\mathbf{R}}_{yy}(n-1) + (1-\alpha)\mathbf{y}(n)\mathbf{y}^{\mathcal{H}}(n). \tag{27}$$

Notice that $\alpha = 0$ corresponds to using the instantaneous correlation matrix estimate $\hat{\mathbf{R}}_{yy}(n) = \mathbf{y}(n)\mathbf{y}^{\mathcal{H}}(n)$ at each iteration. To estimate the covariance matrix $\hat{\mathbf{R}}_{yy}$ more accurately, we can also use forward–backward averaging (see, e.g., [16] for details). This update corresponds to a stochastic gradient algorithm similar to the least mean square (LMS) algorithm that is known to exhibit good tracking performance but will not perform well in the steady state. In contrast, $\alpha = (n-1)/n$ corresponds to the recursive version of the sample estimator in (7) that is expected to yield accurate estimates, so long as the CFO remains time invariant. Note that (27) can also be used with estimates of $\mathbf{R}_{\overline{y}\,\overline{y}}$ that are obtained from $\overline{\mathbf{y}}(n)$ after replacing $\mathbf{y}(n)$ by $\overline{\mathbf{y}}(n)$ in (7).

VI. Simulations

In this section, we will illustrate the identifiability results we obtained in the previous sections through computer simulations that test overall system performance in various scenarios. To this end, we generated three examples using QPSK modulation, fixed and Rayleigh fading channels, and additive white Gaussian noise with zero-mean and variance σ_w^2. The definition of SNR used in these examples is SNR:$= \mathcal{E}^2/\sigma_w^2$ with normalized channel variance; i.e., $\sigma_h^2 = 1$, where $\mathcal{E}^2$ is the energy per symbol.

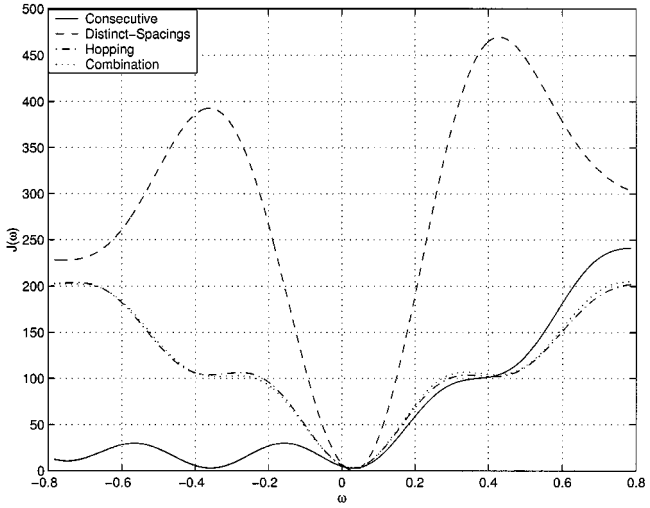

Fig. 2. Cost functions $J(\omega)$ with unique or multiple minima.

Example 1 (Uniqueness): To emphasize the importance of identifiability and to verify the validity of the novel CFO estimators, we construct the following example. We assume that $L = 1$ and choose $K = 13$ (the number of information symbols in each block), and $N = 16$ (the number of symbols in each block after null subcarrier insertion). We consider a deterministic channel realization given by $\mathbf{h} = [1/\sqrt{2},\, j/\sqrt{2}]^T$, with the channel null located at $\rho = \exp(j3\pi/2)$ and fixed CFO at $\omega_o = 0.01\pi$. It can be verified that this channel zero is just on the FFT grid and adjacent with consecutive null subcarriers when one chooses $\mathbf{T}_{\rm sc} = \mathbf{T}_{\rm zp}$. In accordance with Theorem 2, this choice causes $J(\omega)$ to have multiple minima for the method in [10]. In Fig. 2, we depict the cost functions given by (9) to compare the method in [10] (which we term "consecutive" because it employs consecutive null subcarriers), with our methods proposed in Section IV, (which we call "distinct spacings," "hopping," and "combination" for obvious reasons). It can be seen from Fig. 2 that if we put the null subcarriers consecutively at the end of the OFDM block, then $J(\omega)$ does not have a unique minimum. However, we see from the same figure that the approaches outlined in Section IV guarantee the uniqueness of the minimum.

The impact of this identifiability result on average BER and average normalized mean-square-error (MSE) between the CFO estimators and the true CFO are shown in Figs. 3 and 4, respectively. Since the consecutive null subcarrier approach suffers from the nonuniqueness of the minimum, the performance is seen to be worse than the "hopping" or the "combination" or the "distinct spacings" alternatives by at least one order of magnitude at a nominal SNR of 15 dB. Here in Figs. 2–4, we can see that the performance of the "combination" method coincides with that of the "hopping" method. This fact justifies our claim that (18) and (21) are equal.

Example 2 (Rayleigh Fading Channels): In this example, we averaged the BER performance over Rayleigh fading channels. The channel order is $L = 3$, $N = 32$, and $K = 27$. The Gaussian channel taps were chosen randomly and independently (yielding a Rayleigh envelope) with an exponential multipath intensity profile for each of the 300 realizations over

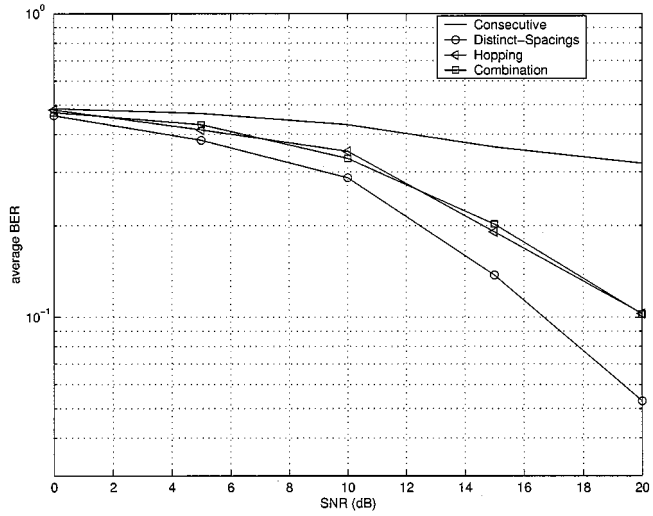

Fig. 3. BER versus SNR (fixed channel).

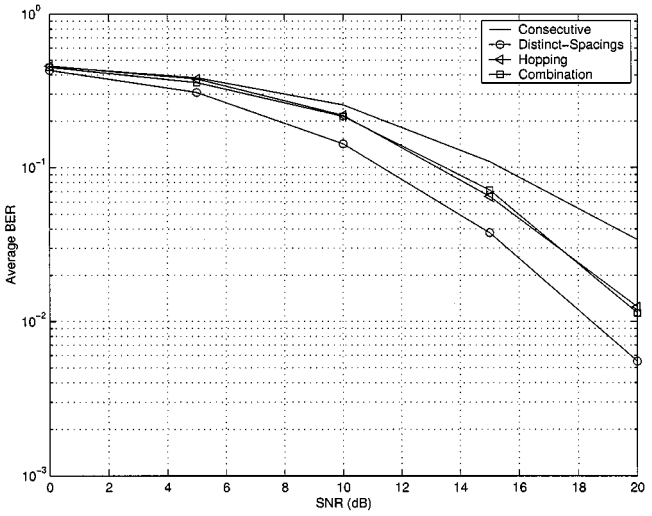

Fig. 5. BER versus SNR (Rayleigh fading channels).

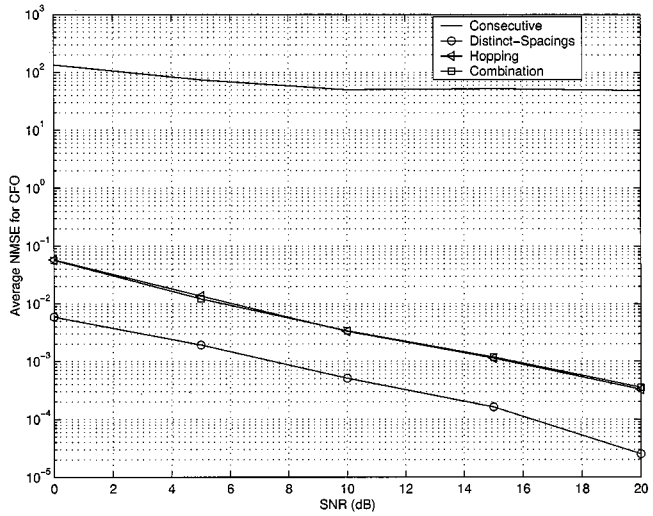

Fig. 4. Normalized MSE versus SNR (fixed channel).

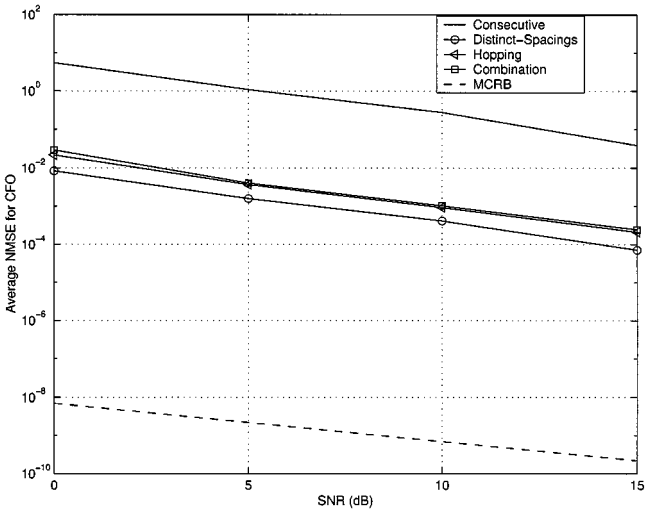

Fig. 6. NMSE versus SNR (Rayleigh fading channels).

which the BER and the normalized MSE were averaged. For fairness, we used the same number of blocks $N_b = 320$ for each method. We see from Fig. 5 that the methods of Section IV outperform that in [10], especially in the high SNR range. And also from Figs. 5 and 6, we can see that the "distinct spacings" method outperforms the "hopping" and the "combination" alternatives with the same number of blocks.

To benchmark performance of the CFO estimators, we also derived the modified Cramér–Rao bound (MCRB) in Appendix B and plotted it with our estimators in Fig. 6 (dashed line). From [13] and [21], we know that the MCRB is lower than both the unconditional CRB (UCRB) and the conditional CRB (CCRB), although it is the most common bound in synchronization theory because of its computational simplicity and the fact that it offers a bound that is not dependent on the particular realization of the symbols. From Fig. 6, we see a big gap between the NMSE curves and the MCRB because 1) the MCRB does not depend on the transmitted symbols deterministically and 2) the average performance over Rayleigh fading channels requires enough blocks of symbols and enough channel realizations. Both 1) and 2) make the MCRB much lower than the CCRB, which is closer to the NMSE. As asserted in [13, p. 56], the CCRB is between the NMSE and MCRB curves. In spite of the gap, we see that above 15 dB, our methods yield an NMSE less than 10^{-4}, which is sufficient to assure reliable BER performance.

Example 3 (LMS performance): In this example, we will illustrate the performance of the LMS-like algorithm of Section V. All the parameters for K, N, L are the same as in Example 2 and the channel is still Rayleigh fading. We choose the step size $\mu(n) = (3/\sqrt{n})N^2\mathcal{E}^2$, where N is the block size, $\mathcal{E}^2$ is the signal energy, and n is the block index. The step size μ is modified in every block since the estimation error of the CFO depends on the value of μ (the closer we come to the true value, the smaller the step size we should choose). The correlation factor $\alpha(n) = (n-1)/n$ is given by (27) since the CFO is a constant in (4). Fig. 7 shows the estimation errors [the difference between $\hat{\omega}(n)$ and ω_o] for three methods. We notice that the adaptive estimators of the CFO fluctuate at the first few iterations, but they converge to the true value at the steady-state. Since the three methods considered in Fig. 7 use the same cost

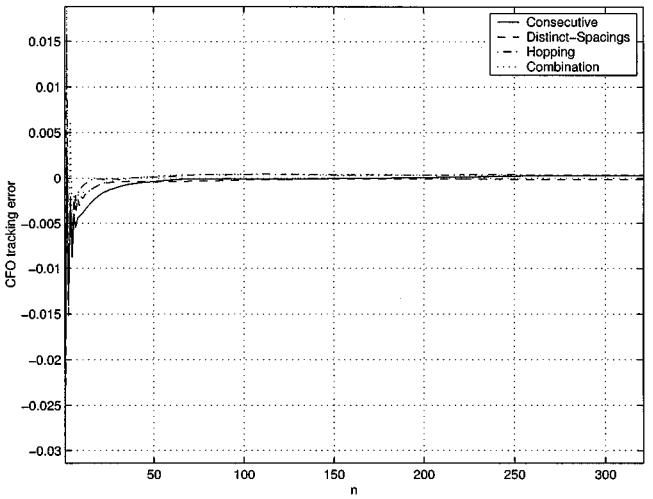

Fig. 7. Adaptive CFO estimation (Rayleigh fading channels).

function and the same number of blocks, they exhibit similar convergence behavior.

VII. Concluding Summary and Future Work

In this paper, we investigated identifiability of non-data-aided schemes for OFDM CFO estimation based on null subcarriers, paying special attention to the possibility of channel nulls. We showed that the conventional approaches of [10] and [20] might suffer from channel zeros on the FFT grid and proposed a new approach where the null subcarriers are placed with distinct spacings. We also studied the null subcarrier hopping approach of [1] by expressing it in terms of our matrix-vector model for the CFO estimation problem in single-user OFDM transmissions and by proving that indeed, hopping guarantees that $J(\omega)$ has a unique minimum. We also adopted a low-complexity LMS-like adaptive gradient descent method for finding the minimum of $J(\omega)$ that can be implemented online. Computer simulations corroborated the impact of our identifiability results on system performance.

In terms of future directions, it would be interesting to explore how pilot carriers can be utilized to perform joint channel and CFO estimation. In this context, other issues such as the optimal placement of pilots to enhance the estimator performance remain to be explored.

Appendix A
Proof of Theorem 1

From (6), we see that it suffices to show that $\mathbf{B}_F\mathbf{R}_{ss}\mathbf{B}_F^{\mathcal{H}} = \mathbf{B}'_F\mathbf{R}_{ss}\mathbf{B}'^{\mathcal{H}}_F$, where $\mathbf{B}_F := \mathbf{D}_N(\omega_o)\mathbf{F}_N^{\mathcal{H}}\mathbf{T}_{\rm zp}\ \mathbf{D}_K(\tilde{\mathbf{h}})$ and $\mathbf{B}'_F := \mathbf{D}_N(\omega'_o)\mathbf{F}_N^{\mathcal{H}}\mathbf{T}_{\rm zp}\mathbf{D}_K(\tilde{\mathbf{h}}')$. We will provide a constructive proof. Let $\omega_o = 0$, $\omega'_o = 2\pi/N$ and define $\mathbf{h} := [h(0)\cdots h(L)]^T$, and likewise for $\mathbf{h}'$. Expressing the Fourier transforms of $\mathbf{h}$ and $\mathbf{h}'$ in matrix form, we can write: $\tilde{\mathbf{h}} = \mathbf{F}_{K\times(L+1)}\mathbf{h}$ and $\tilde{\mathbf{h}}' = \mathbf{F}_{K\times(L+1)}\mathbf{h}'$, where $\mathbf{F}_{K\times(L+1)}$ consists of the first K rows and $L+1$ columns of $\mathbf{F}_N$. Select $\mathbf{h}$ to have taps with zero sample mean, or, equivalently with zero dc; i.e., choose $\mathbf{h}$ such that $[\mathbf{F}_{K\times(L+1)}\mathbf{h}]_1 := \mathbf{f}_{L+1}^{\mathcal{H}}(0)\mathbf{h} = [1\cdots 1]\mathbf{h} = 0$, which implies that the Fourier transform vector is expressed as $\tilde{\mathbf{h}} = [0\ \mathbf{b}^T]^T$, for some $(K-1)\times 1$ vector $\mathbf{b}$. Also, choose $\mathbf{h}$ to have zero frequency response at $2\pi K/N$; i.e., $\mathbf{f}_{L+1}^{\mathcal{H}}(2\pi K/N)\mathbf{h} = 0$. Finally, select $\mathbf{h}'$ to be a modulated version of $\mathbf{h}$ as follows: $\mathbf{h}' = \mathbf{D}_{L+1}^{\mathcal{H}}(\omega'_o)\mathbf{h}$, where $\omega'_o = 2\pi/N$. Recalling that $\tilde{\mathbf{h}} = [0\ \mathbf{b}^T]^T$, we thus infer that $\tilde{\mathbf{h}}' = [\mathbf{b}^T\ \mathbf{f}_{L+1}^{\mathcal{H}}(2\pi K/N)\mathbf{h}]^T = [\mathbf{b}^T\ 0]^T$. Now we can verify by direct substitution of these $\tilde{\mathbf{h}}$ and $\tilde{\mathbf{h}}'$ to the definitions of $\mathbf{B}_F$ and $\mathbf{B}'_F$ that

$$\mathbf{B}_F = \left[\mathbf{0}\ \ [\mathbf{b}]_1\mathbf{f}_N\left(\frac{2\pi}{N}\right)\cdots[\mathbf{b}]_{K-1}\mathbf{f}_N\left(\frac{2\pi(K-1)}{N}\right)\right]$$

$$\mathbf{B}'_F = \left[[\mathbf{b}]_1\mathbf{f}_N\left(\frac{2\pi}{N}\right)\cdots[\mathbf{b}]_{K-1}\mathbf{f}_N\left(\frac{2\pi(K-1)}{N}\right)\ \ \mathbf{0}\right]. \quad (28)$$

Recall that we want to show that $\mathbf{B}_F\mathbf{R}_{ss}\mathbf{B}_F^{\mathcal{H}} = \mathbf{B}'_F\mathbf{R}_{ss}\mathbf{B}'^{\mathcal{H}}_F$, for the chosen $(\omega_o, h(l))$ and $(\omega'_o, h'(l))$ to yield the same covariance matrix. But using (28), we can obtain the following:

$$\mathbf{B}_F\mathbf{R}_{ss}\mathbf{B}_F^{\mathcal{H}} = \sum_{i=1}^{K-1}\sum_{k=1}^{K-1}[\mathbf{b}]_i\mathbf{f}_N\left(\frac{2\pi i}{N}\right)[\mathbf{R}_{ss}]_{i+1,\,k+1}\,\mathbf{f}_N^{\mathcal{H}}\left(\frac{2\pi i}{N}\right)[\mathbf{b}]_k,$$

$$\mathbf{B}'_F\mathbf{R}_{ss}\mathbf{B}'^{\mathcal{H}}_F = \sum_{i=1}^{K-1}\sum_{k=1}^{K-1}[\mathbf{b}]_i\mathbf{f}_N\left(\frac{2\pi i}{N}\right)[\mathbf{R}_{ss}]_{i,\,k}\,\mathbf{f}_N^{\mathcal{H}}\left(\frac{2\pi i}{N}\right)[\mathbf{b}]_k. \quad (29)$$

And since $\mathbf{R}_{ss}$ is a Toeplitz matrix, we have $[\mathbf{R}_{ss}]_{i,k} = [\mathbf{R}_{ss}]_{i+1,k+1}$; hence, $\mathbf{B}_F\mathbf{R}_{ss}\mathbf{B}_F^{\mathcal{H}} = \mathbf{B}'_F\mathbf{R}_{ss}\mathbf{B}'^{\mathcal{H}}_F$, which completes the proof of the theorem. ■

Appendix B
Modified Cramér–Rao Bound

In this Appendix, we will derive the MCRB for the CFO estimator based on the data model in (4). Since the noise $\mathbf{v}(n)$ contains zero mean independent identically distributed complex Gaussian random variables that are also uncorrelated from the symbols $\mathbf{s}(n)$, the joint probability density function of $\mathbf{Y} := [\mathbf{y}(0), \mathbf{y}(1), \ldots, \mathbf{y}(N_b-1)]$ is given by

$$p_{\mathbf{Y}|\omega_o,\,\mathbf{h},\,\mathbf{S}}(\mathbf{Y}|\omega_o,\,\mathbf{h},\,\mathbf{S}) = \frac{1}{(2\pi)^{N_bN}\sigma_v^{2N_bN}} \cdot \exp\left(-\frac{1}{\sigma_v^2}\sum_{n=0}^{N_b-1}\left\|\mathbf{y}(n) - e^{j\omega_o(nP+\overline{L})}\mathbf{D}_N(\omega_o)\cdot\mathbf{H}\mathbf{F}_N^{\mathcal{H}}\mathbf{T}_{\rm sc}\mathbf{s}(n)\right\|^2\right) \quad (30)$$

where $\mathbf{S} := [\mathbf{s}(0), \mathbf{s}(1), \ldots, \mathbf{s}(N_b-1)]$. Define the circulant matrix $\mathbf{H}$ in (4) as $\mathbf{H} = \sum_{l=0}^{L}h(l)\mathbf{P}_l$, where $\mathbf{P}_i$ is a circulant matrix with entries $[\mathbf{P}_i]_{l,\,k} = \delta[k-l-i \bmod N]$, and $\delta[i]$ denotes Kronecker's delta. For N_b blocks, the log-likelihood function $f(\boldsymbol{\theta}, \mathbf{S}) := \ln p(\mathbf{Y}|\omega_o, \mathbf{h}, \mathbf{S})$ can be written as

$$f(\boldsymbol{\theta}, \mathbf{S}) = -N_bN\ln(2\pi\sigma_v^2) - \frac{1}{\sigma_v^2}\sum_{n=0}^{N_b-1}\cdot\left\|\mathbf{y}(n) - e^{j\omega_o(Pn+\overline{L})}\mathbf{D}(\omega_o)\mathbf{H}\mathbf{F}_N^{\mathcal{H}}\mathbf{T}_{\rm sc}\mathbf{s}(n)\right\|^2 \quad (31)$$

$$\mathcal{J}_{1,1} = \frac{2}{\sigma_v^2} \sum_{n=0}^{N_b-1} \mathrm{tr}\left(\mathbf{D}(n)\mathbf{H}\mathbf{F}_N^{\mathcal{H}}\mathbf{T}_{\mathrm{sc}}\mathbf{R}_{ss}\mathbf{T}_{\mathrm{sc}}^{\mathcal{H}}\mathbf{F}_N\mathbf{H}^{\mathcal{H}}\mathbf{D}(n)\right)$$

$$\boldsymbol{\mathcal{J}}_{1,2} = -\frac{j}{\sigma_v^2} \sum_{n=0}^{N_b-1} \left[\mathrm{tr}\left(\mathbf{P}_0\mathbf{F}_N^{\mathcal{H}}\mathbf{T}_{\mathrm{sc}}\mathbf{R}_{ss}\mathbf{T}_{\mathrm{sc}}^{\mathcal{H}}\mathbf{F}_N\mathbf{H}^{\mathcal{H}}\mathbf{D}(n)\right), \ldots, \mathrm{tr}\left(\mathbf{P}_L\mathbf{F}_N^{\mathcal{H}}\mathbf{T}_{\mathrm{sc}}\mathbf{R}_{ss}\mathbf{T}_{\mathrm{sc}}^{\mathcal{H}}\mathbf{F}_N\mathbf{H}^{\mathcal{H}}\mathbf{D}(n)\right)\right]$$

$$\boldsymbol{\mathcal{J}}_{2,2} = \frac{1}{\sigma_v^2} \sum_{n=0}^{N_b-1} \begin{pmatrix} \mathrm{tr}\left(\mathbf{P}_0\mathbf{F}_N^{\mathcal{H}}\mathbf{T}_{\mathrm{sc}}\mathbf{R}_{ss}\mathbf{T}_{\mathrm{sc}}^{\mathcal{H}}\mathbf{F}_N\mathbf{P}_0^T\right) & \cdots & \mathrm{tr}\left(\mathbf{P}_L\mathbf{F}_N^{\mathcal{H}}\mathbf{T}_{\mathrm{sc}}\mathbf{R}_{ss}\mathbf{T}_{\mathrm{sc}}^{\mathcal{H}}\mathbf{F}_N\mathbf{P}_0^T\right) \\ \vdots & \vdots & \vdots \\ \mathrm{tr}\left(\mathbf{P}_0\mathbf{F}_N^{\mathcal{H}}\mathbf{T}_{\mathrm{sc}}\mathbf{R}_{ss}\mathbf{T}_{\mathrm{sc}}^{\mathcal{H}}\mathbf{F}_N\mathbf{P}_L^T\right) & \cdots & \mathrm{tr}\left(\mathbf{P}_L\mathbf{F}_N^{\mathcal{H}}\mathbf{T}_{\mathrm{sc}}\mathbf{R}_{ss}\mathbf{T}_{\mathrm{sc}}^{\mathcal{H}}\mathbf{F}_N\mathbf{P}_L^T\right) \end{pmatrix}. \quad (36)$$

where the equivalent $1 \times (1+2(L+1))$ complex parameter vector $\boldsymbol{\theta} := [\omega_o, \mathbf{h}^T, \mathbf{h}^{\mathcal{H}}]^T$ includes the unknown CFO as well as the channel and its conjugate. From [21], the MCRB is defined as

$$\mathrm{MCRB}(\boldsymbol{\theta}) := \boldsymbol{\mathcal{J}}^{-1}(\boldsymbol{\theta}) := E_{\mathbf{Y},\mathbf{S}}\left\{\left(\frac{\partial f(\boldsymbol{\theta},\mathbf{S})}{\partial\boldsymbol{\theta}}\right)^{\mathcal{H}}\left(\frac{\partial f(\boldsymbol{\theta},\mathbf{S})}{\partial\boldsymbol{\theta}}\right)\right\}^{-1} \quad (32)$$

where $\boldsymbol{\mathcal{J}}(\boldsymbol{\theta})$ is the so-called Fisher's information matrix (FIM). Taking partial derivatives of $f(\boldsymbol{\theta},\mathbf{S})$ with respect to the unknown parameters, we obtain

$$\frac{\partial f(\boldsymbol{\theta},\mathbf{S})}{\partial\omega_o} = -\frac{2}{\sigma_v^2}\sum_{n=0}^{N_b-1}\Im\left(e^{j\omega_o(nP+\overline{L})}\mathbf{v}^{\mathcal{H}}(n)\mathbf{D}(n)\mathbf{D}(\omega_o)\cdot\mathbf{H}\mathbf{F}_N^{\mathcal{H}}\mathbf{T}_{\mathrm{sc}}\mathbf{s}(n)\right)$$

$$\frac{\partial f(\boldsymbol{\theta},\mathbf{S})}{\partial h(l)} = \frac{1}{\sigma_v^2}\sum_{n=0}^{N_b-1}\mathbf{v}^{\mathcal{H}}(n)\cdot\left(e^{j\omega_o(nP+\overline{L})}\mathbf{D}(\omega_o)\mathbf{P}_l\mathbf{F}_N^{\mathcal{H}}\mathbf{T}_{\mathrm{sc}}\mathbf{s}(n)\right), \quad \forall l\in[0,L] \quad (33)$$

where $\mathbf{D}(n) := \mathrm{diag}\{Pn+\overline{L}, Pn+\overline{L}+1, \ldots, Pn+\overline{L}+N-1\}$. Furthermore, we find

$$E_{\mathbf{Y},\mathbf{S}}\left\{\frac{\partial f(\boldsymbol{\theta},\mathbf{S})}{\partial\omega_o}\frac{\partial f(\boldsymbol{\theta},\mathbf{S})}{\partial\omega_o}\right\} = \frac{2}{\sigma_v^2}\sum_{n=0}^{N_b-1}\mathrm{tr}\left(\mathbf{D}(n)\mathbf{H}\mathbf{F}_N^{\mathcal{H}}\mathbf{T}_{\mathrm{sc}}\mathbf{R}_{ss}\mathbf{T}_{\mathrm{sc}}^{\mathcal{H}}\mathbf{F}_N\mathbf{H}^{\mathcal{H}}\mathbf{D}(n)\right)$$

$$E_{\mathbf{Y},\mathbf{S}}\left\{\frac{\partial f(\boldsymbol{\theta},\mathbf{S})}{\partial h^*(k)}\frac{\partial f(\boldsymbol{\theta},\mathbf{S})}{\partial h(l)}\right\} = \frac{1}{\sigma_v^2}\sum_{n=0}^{N_b-1}\mathrm{tr}\left(\mathbf{P}_l\mathbf{F}_N^{\mathcal{H}}\mathbf{T}_{\mathrm{sc}}\mathbf{R}_{ss}\mathbf{T}_{\mathrm{sc}}^{\mathcal{H}}\mathbf{F}_N\mathbf{P}_k^T\right)$$

$$E_{\mathbf{Y},\mathbf{S}}\left\{\frac{\partial f(\boldsymbol{\theta},\mathbf{S})}{\partial\omega_o}\frac{\partial f(\boldsymbol{\theta},\mathbf{S})}{\partial h(l)}\right\} = -\frac{j}{\sigma_v^2}\sum_{n=0}^{N_b-1}\mathrm{tr}\left(\mathbf{D}(n)\mathbf{P}_l\mathbf{F}_N^{\mathcal{H}}\mathbf{T}_{\mathrm{sc}}\mathbf{R}_{ss}\mathbf{T}_{\mathrm{sc}}^{\mathcal{H}}\mathbf{F}_N\mathbf{H}^{\mathcal{H}}\right)$$

$$E_{\mathbf{Y},\mathbf{S}}\left\{\frac{\partial f(\boldsymbol{\theta},\mathbf{S})}{\partial\omega_o}\frac{\partial f(\boldsymbol{\theta},\mathbf{S})}{\partial h^*(l)}\right\} = \left(E_{\mathbf{Y},\mathbf{S}}\left\{\frac{\partial f(\boldsymbol{\theta},\mathbf{S})}{\partial\omega_o}\frac{\partial f(\boldsymbol{\theta},\mathbf{S})}{\partial h(l)}\right\}\right)^*$$

$$E_{\mathbf{Y},\mathbf{S}}\left\{\frac{\partial f(\boldsymbol{\theta},\mathbf{S})}{\partial h^*(l)}\frac{\partial f(\boldsymbol{\theta},\mathbf{S})}{\partial h^*(k)}\right\} = E_{\mathbf{Y},\mathbf{S}}\left\{\frac{\partial f(\boldsymbol{\theta},\mathbf{S})}{\partial h(l)}\frac{\partial f(\boldsymbol{\theta},\mathbf{S})}{\partial h(k)}\right\} = 0, \quad \forall k,l\in[0,L] \quad (34)$$

where $\mathrm{tr}(\mathbf{D})$ denotes the trace of $\mathbf{D}$. The equivalent FIM and the MCRB of the CFO ($\mathcal{C}_o$) based on the model (4) are given by

$$\boldsymbol{\mathcal{J}}(\boldsymbol{\theta}) = \begin{pmatrix} \mathcal{J}_{1,1} & \boldsymbol{\mathcal{J}}_{1,2} & \boldsymbol{\mathcal{J}}_{1,2}^* \\ \boldsymbol{\mathcal{J}}_{1,2}^{\mathcal{H}} & \boldsymbol{\mathcal{J}}_{2,2} & \mathbf{0} \\ \boldsymbol{\mathcal{J}}_{1,2}^T & \mathbf{0} & \boldsymbol{\mathcal{J}}_{2,2} \end{pmatrix}$$

$$\mathcal{C}_o = \left(\mathcal{J}_{1,1} - 2\Re\left(\boldsymbol{\mathcal{J}}_{1,2}\boldsymbol{\mathcal{J}}_{2,2}^{-1}\boldsymbol{\mathcal{J}}_{1,2}^{\mathcal{H}}\right)\right)^{-1} \quad (35)$$

where in deriving the MCRB, we used the inversion property of block matrices,[3] and $\mathcal{J}_{1,1}$, $\boldsymbol{\mathcal{J}}_{1,2}$ and $\boldsymbol{\mathcal{J}}_{2,2}$ are given in (36), shown at the top of the page.

REFERENCES

[1] S. Barbarossa, M. Pompili, and G. B. Giannakis, "Timing and frequency synchronization of orthogonal frequency multiple access systems," in *Proc. Int. Conf. Communications*, vol. 6, Helsinki, Finland, June 11–15, 2001, pp. 1674–1678.

[2] J. van de Beek, M. Sandell, and P. O. Börjesson, "ML estimation of time and frequency offset in OFDM systems," *IEEE Trans. Signal Processing*, vol. 45, pp. 1800–1805, July 1997.

[3] H. Bolcskei, "Blind high-resolution uplink synchronization of OFDM-based multiple access schemes," in *Proc. IEEE Workshop Signal Processing Advances in Wireless Communications*, Annapolis, MD, 1999, pp. 166–169.

[4] F. Classen and H. Meyr, "Frequency synchronization algorithms for OFDM systems suitable for communication over frequency-selective fading channels," in *Proc. Vehicular Tech. Conf.*, vol. 3, 1994, pp. 1655–1659.

[5] ETSI Normalization Committee, "Channel models for HIPERLAN/2 in different indoor scenarios," European Telecommunications Standards Institute, Sophia-Antipolis, Valbonne, France, Norme ETSI, doc. 3ERI085B, 1998.

[3]For matrices of compatible dimensions, the following holds:

$$\begin{pmatrix}\mathbf{A} & \mathbf{B}\\ \mathbf{C} & \mathbf{D}\end{pmatrix}^{-1} = \begin{pmatrix}\mathbf{X} & -\mathbf{X}\mathbf{B}\mathbf{D}^{-1}\\ -\mathbf{D}^{-1}\mathbf{C}\mathbf{X} & \mathbf{D}^{-1}(\mathbf{I}+\mathbf{C}\mathbf{X}\mathbf{B}\mathbf{D}^{-1})\end{pmatrix}$$

where $\mathbf{X} = (\mathbf{A}-\mathbf{B}\mathbf{D}^{-1}\mathbf{C})^{-1}$.

[6] G. H. Golub and C. F. van Loan, *Matrix Computations*, 3rd ed. Baltimore, MD: Johns Hopkins Univ. Press, 1996.
[7] *Wireless LAN Medium Access Control (MAC) and Physical Layer (PHY) Specifications*, Sept. 1999.
[8] S. Kapoor, D. J. Marchok, and Y.-F. Huang, "Pilot assisted synchronization for wireless OFDM using pilot carriers," in *Proc. Vehicular Technol. Conf.*, vol. 3, 1998, pp. 2077–2080.
[9] N. Lashkarian and S. Kiaei, "Class of cyclic-based estimators for frequency-offset estimation of OFDM systems," *IEEE Trans. Commun.*, vol. 48, pp. 2139–2149, Dec. 2000.
[10] H. Liu and U. Tureli, "A high efficiency carrier estimator for OFDM communications," *IEEE Commun. Lett.*, vol. 2, pp. 104–106, Apr. 1998.
[11] M. Luise and R. Reggiannini, "Carrier frequency offset acquisition and tracking for OFDM systems," *IEEE Trans. Commun.*, vol. 44, pp. 1590–1598, Nov. 1996.
[12] X. Ma, G. B. Giannakis, and S. Barbarossa, "Non-data-aided frequency-offset and channel estimation in OFDM and related block transmissions," in *Proc. Int. Conf. Communications*, vol. 6, Helsinki, Finland, June 11–15, 2001, pp. 1866–1870.
[13] U. Mengali and A. D'Andrea, *Synchronization Techniques for Digital Receivers*. New York: Plenum, 1997.
[14] M. Morelli and U. Mengali, "An improved frequency offset estimator for OFDM applications," *IEEE Commun. Lett.*, vol. 3, pp. 75–77, Mar. 1999.
[15] P. H. Moose, "A technique for orthogonal frequency division multiplexing frequency offset correction," *IEEE Trans. Commun.*, vol. 42, pp. 2908–2914, Oct. 1994.
[16] M. Pesavento, A. B. Gershman, and M. Haardt, "Unitary root-MUSIC with a real-valued eigendecomposition: A theoretical and experimental performance study," *IEEE Trans. Signal Processing*, vol. 48, pp. 1306–1314, May 2000.
[17] T. Pollet, M. Van Bladel, and M. Moenaclaey, "BER sensitivity of OFDM systems to carrier frequency offset and Wiener phase noise," *IEEE Trans. Commun.*, vol. 43, pp. 191–192, Feb./Mar./Apr. 1995.
[18] T. M. Schmidl and D. C. Cox, "Robust frequency and timing synchronization for OFDM," *IEEE Trans. Commun.*, vol. 45, no. 12, pp. 1613–1621, Dec. 1997.
[19] P. Stoica and T. Söderström, "Statistical analysis of MUSIC and subspace rotation estimates of sinusoidal frequencies," *IEEE Trans. Signal Processing*, vol. 39, pp. 1836–1847, Aug. 1991.
[20] U. Tureli, H. Liu, and M. D. Zoltowski, "OFDM blind carrier offset estimation: ESPRIT," *IEEE Trans. Commun.*, vol. 48, pp. 1459–1461, Sept. 2000.
[21] G. Vazquez and J. Riba, "Non-data-aided digital synchronization," in *Signal Processing Advances in Wireless & Mobile Communications*, G. B. Giannakis, Y. Hua, P. Stoica, and L. Tong, Eds. Englewood Cliffs, NJ: Prentice-Hall, 2000, vol. 2, ch. 9, pp. 357–402.
[22] Z. Wang and G. B. Giannakis, "Wireless multicarrier communications: Where Fourier meets Shannon," *IEEE Signal Processing Mag.*, vol. 17, pp. 29–48, May 2000.
[23] S. Zhou and G. B. Giannakis, "Finite-alphabet based channel estimation for OFDM and related multi-carrier systems," *IEEE Trans. Commun.*, vol. 49, pp. 1402–1414, Aug. 2001.

Xiaoli Ma received the B.S. degree in automatic control from Tsinghua University, China, in 1998 and the M.S. degree in electrical engineering from the University of Virginia, Charlottesville, in 1999. She is currently pursuing the Ph.D. degree at the Department of Electrical and Computer Engineering, University of Minnesota, Minneapolis.

Her current research interests include carrier synchronization for OFDM systems, transmitter and receiver diversity techniques for fading channels, communications over time- and frequency-selective channels, channel estimation, and equalization algorithms.

Cihan Tepedelenlioğlu (M'01) was born in Ankara, Turkey, in 1973. He received the B.S. degree (with highest honors) from the Florida Institute of Technology, Melbourne, in 1995 and the M.S. degree from the University of Virginia, Charlottesville, in 1998, both in electrical engineering. He received the Ph.D. degree in electrical and computer engineering from the University of Minnesota, Minneapolis, in 2001.

He is currently an Assistant Professor of electrical engineering at the Telecommunications Research Center, Arizona State University, Tempe. From January 1999 to May 2001, he was a Research Assistant at the University of Minnesota. His research interests include statistical signal processing; system identification; wireless communications; estimation and equalization algorithms for wireless systems, filterbanks, and multirate systems; carrier synchronization for OFDM systems; power estimation; and handoff algorithms.

Georgios B. Giannakis (F'97) received the diploma in electrical engineering from the National Technical University of Athens, Greece, in 1981. He received the M.Sc. degree in electrical engineering, the M.Sc. degree in mathematics, and the Ph.D. degree in electrical engineering from the University of Southern California (USC), Los Angeles, in 1983, 1986, and 1986, respectively.

After lecturing for one year at USC, he joined the University of Virginia in 1987, where he became a Professor of electrical engineering in 1997. Since 1999, he has been a Professor with the Department of Electrical and Computer Engineering, University of Minnesota, Minneapolis, where he now holds an ADC Chair in wireless telecommunications. His general interests span the areas of communications and signal processing, estimation and detection theory, time-series analysis, and system identification—subjects on which he has published more than 125 journal papers, 250 conference papers, and two edited books. His current research topics focus on transmitter and receiver diversity techniques for single- and multiuser fading communication channels, redundant precoding, and space–time coding for block transmissions, multicarrier, and wide-band wireless communication systems. He a frequent Consultant for the telecommunications industry.

Prof. Giannakis is the Corecipient of three Best Paper Awards from the IEEE Signal Processing (SP) Society (1992, 1998, 2000). He also received the society's Technical Achievement Award in 2000. He coorganized three IEEE-SP Workshops (HOS in 1993, SSAP in 1996, and SPAWC in 1997) and guest coedited four special issues. He was an Associate Editor for the IEEE TRANSACTIONS ON SIGNAL PROCESSING and the IEEE SIGNAL PROCESSING LETTERS. He was a Secretary of the SP Conference Board, a Member of the SP Publications Board, and a Member and Vice-chair of the Statistical Signal and Array Processing Committee. He is a Member of the Editorial Board for the PROCEEDINGS OF THE IEEE. He chairs the SP for Communications Technical Committee and is the Editor in Chief for the IEEE SIGNAL PROCESSING LETTERS. He is a member of the IEEE Fellows Election Committee and the IEEE-SP Society's Board of Governors.

Sergio Barbarossa (M'88) graduated cum laude in electrical engineering from the University of Rome "La Sapienza" in 1984 and he received his Ph.D. degree from the same university in 1989. He joined the Radar System Division of Selenia in 1985 as a radar system engineer. From November 1987 to August 1988 he was a Research Engineer at the Environmental Research Institute of Michigan (ERIM), Ann Arbor (USA), where he was involved in research activities on Synthetic Aperture Radars. After three years at the University of Perugia as Adjunct Professor, in 1991 he joined the University of Rome "La Sapienza" where he is now a Full Professor. He has held positions as visiting scientist at the University of Virginia in the springs of 1995 and 1997, and as visiting professor at the University of Minnesota in 1999. He has served as an Associate Editor for the IEEE TRANSACTIONS ON SIGNAL PROCESSING and, since 1997, he is a member of the IEEE Signal Processing for Communications Technical Committee. He has received the 2000 IEEE Best Paper Award for a paper published in the IEEE TRANSACTIONS ON SIGNAL PROCESSING, co-authored with A. Scaglione and G. B. Giannakis. He is currently leading the University of Rome's team involved in two international projects supported by the European Community on wireless communications involving space-time coding and code division multiple access. His current research interests include multiple access methods, space-time coding, communications over time-varying channels.